Motueka: Composition and Sources of $PM_{2.5}$

PK Davy WJ Trompetter

GNS Science Consultancy Report 2023/77
November 2023

DISCLAIMER

This report has been prepared by the Institute of Geological and Nuclear Sciences Limited (GNS Science) exclusively for and under contract to Tasman District Council. Unless otherwise agreed in writing by GNS Science, GNS Science accepts no responsibility for any use of or reliance on any contents of this report by any person other than Tasman District Council and shall not be liable to any person other than Tasman District Council, on any ground, for any loss, damage or expense arising from such use or reliance.

Use of Data:

Date that GNS Science can use associated data: November 2023

BIBLIOGRAPHIC REFERENCE

Davy PK, Trompetter WJ. 2023. Motueka: composition and sources of $PM_{2.5}$. Lower Hutt (NZ): GNS Science. 46 p. Consultancy Report 2023/77.

CONTENTS

FIGURES

TABLES

APPENDICES

APPENDIX FIGURES

APPENDIX TABLES

EXECUTIVE SUMMARY

This report presents the results of an analysis of particulate matter concentrations and composition from a year-long $PM_{2.5}$ sampling campaign at Motueka in Tasman District. Particulate matter samples were collected on a daily basis from January 2022 to January 2023. The compositional data has been used in a receptor modelling study to apportion particulate matter emission sources contributing to ambient particulate matter concentrations in the township. Understanding the sources of fine-particle air pollution is important for air-quality management and the prevention of health impacts on exposed populations.

Key results from the study are:

1. Fine-particle concentrations were highest during winter, and this was indicative of the sources contributing to particulate matter concentrations at Motueka.
2. Five distinct source types were extracted from the data; these were: biomass combustion, motor vehicles, secondary sulphate, marine aerosol (sea salt) and soil.
3. Biomass combustion was the primary source of fine particulate matter in Motueka, contributing to 64% of $PM_{2.5}$ over the monitoring period, with most of this occurring during winter. The contribution from this source on peak pollution days was found to be 87% of $PM_{2.5}$ concentrations. Trace amounts of arsenic (As) and lead (Pb) were found to be associated with the biomass combustion source, most likely due to the use of treated (copper chrome arsenate [CCA]-treated and old painted timber) fuel for domestic fires during winter.

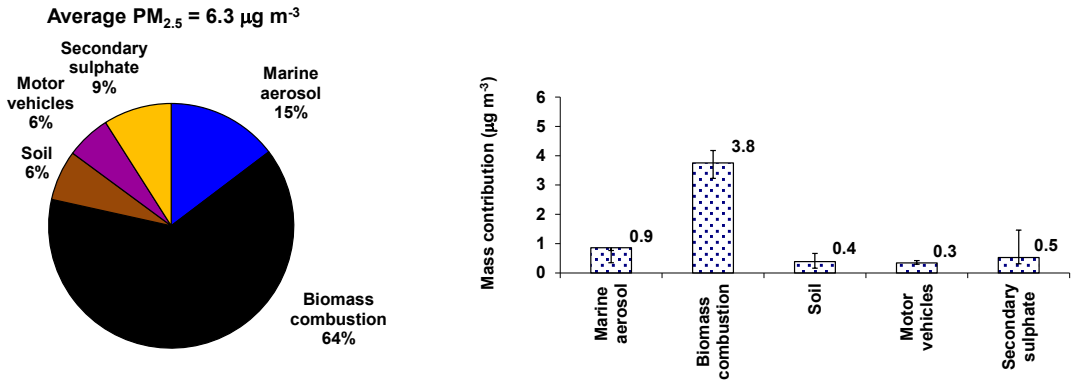

Figure ES.1 Average source contributions to $PM_{2.5}$ at Motueka over the monitoring period (January 2022 to January 2023).

During other time periods, marine aerosol, secondary sulphate and crustal matter contributions can be significant. The motor vehicle source contributed low levels of $PM_{2.5}$ during the monitoring period, most likely due to the low level of traffic activity near the Motueka monitoring site.

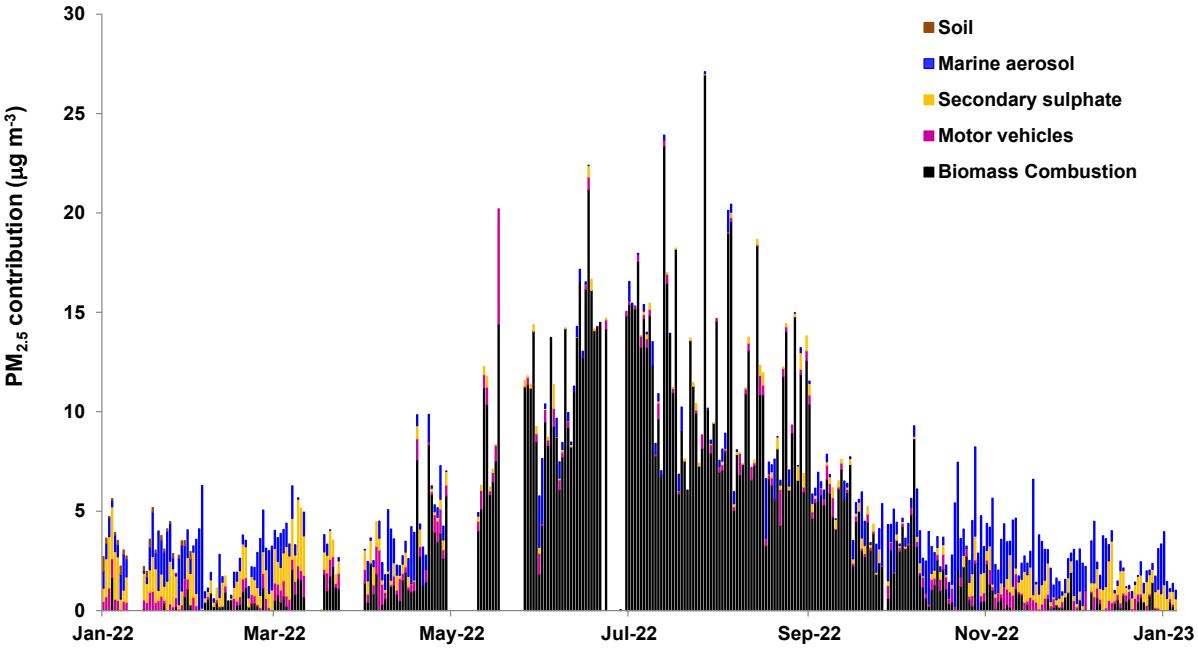

Figure ES.2 Daily source contributions to $PM_{2.5}$ at Motueka over the monitoring period (January 2022 to January 2023).

This page left intentionally blank.

1.0 INTRODUCTION

This report presents the results of a compositional analysis and receptor modelling study of airborne particle samples collected during 2022 at a council-operated ambient air quality monitoring site in Motueka, Tasman District. The work was commissioned by Tasman District Council (TDC) as part of its ambient air-quality monitoring programme and the requirement to manage air quality in the Tasman region.

1.1 Requirement to Manage Airborne Particle Pollution

In response to growing evidence of significant health effects associated with airborne particle pollution, the New Zealand Government introduced in 2004 a National Environmental Standard (NES) of 50 μg/m^3 for particles less than 10 μm in aerodynamic cross-section (denoted as PM_{10}). The NES places the onus on regional councils to monitor PM_{10} and publicly report whether the air quality in their region exceeds the standard, with a provision for no more than one exceedance annually plus exceptional events by application for exemption (e.g. dust storms, volcanic eruptions) and a requirement for offsets by industry in PM_{10}-polluted airsheds replacing the restriction on industrial consents (Ministry for the Environment 2011).

Clearly then, in areas where the PM_{10} standard is exceeded, information on the sources contributing to those air pollution episodes is required in order to:

- identify ‘exceptional events’ outside of regulatory authority control
- effectively manage air quality, and
- formulate appropriate mitigation strategies where necessary.

In addition to the PM_{10} NES, the Ministry for the Environment issued ambient air-quality guidelines for air pollutants in 2002 that included a (monitoring) guideline value of 25 μg m^{-3} for $PM_{2.5}$ (24-hour average). More recently, the World Health Organisation (WHO) has recently confirmed a $PM_{2.5}$ ambient air-quality guideline value of 15 μg m^{-3} (24-hour average) based on the relationship between 24-hour and annual particulate matter levels (WHO 2021). The WHO annual average guideline for $PM_{2.5}$ is 5 μg m^{-3}. These are the lowest levels at which total, cardiopulmonary and lung cancer mortality have been shown to increase, with more than 95% confidence in response to exposure to $PM_{2.5}$. WHO recommends the use of $PM_{2.5}$ guidelines over PM_{10}, as epidemiological studies have shown that most of the adverse health effects associated with PM_{10} are due to $PM_{2.5}$.

1.1.1 Identifying Sources of Airborne Particle Pollution

Measuring the mass concentration of air particulate matter provides little information on the identity of the contributing sources. Airborne particles are composed of many elements and compounds from many different sources. Receptor modelling provides a means to determine the relative mass contribution of sources that impact significantly on the total mass of air particulate matter collected at a monitoring site. Elemental concentrations in particulate matter filter samples were determined using X-ray fluorescence spectroscopy (XRF) at the New Zealand Ion Beam Analysis Facility in Gracefield, Lower Hutt. Black carbon concentrations were determined using light reflection techniques.

XRF is a mature analytical technique that provides a non-destructive determination of multi-elemental concentrations present in a sample. Using elemental concentrations with appropriate statistical techniques and purpose-designed mathematical models, the sources contributing to each ambient sample can be estimated. Appendix 1 provides a description of the XRF analytical process and receptor modelling techniques.

1.1.2 Scope of this Study

This report describes the sampling, results and outcomes according to the following objectives:

- Identify the sources contributing to air pollution episodes.
- Identify the sources responsible for the emission of toxic contaminants.
- Estimate the contribution of sea salt and other natural particulate-matter sources to ambient concentrations.
- Estimate the contribution of secondary particulate matter sources to ambient concentrations.
- Distinguish between the contribution of home heating and motor vehicle emission sources.
- Determine the variation of source contributions by season.

2.0 METHODOLOGY

2.1 Location of the Motueka Particulate Matter Speciation Monitoring Site

Particulate matter ($PM_{2.5}$) sampling was undertaken by TDC from January 2022 until January 2023 at its temporary air-quality monitoring station on the grounds of Ledger Goodman Park, Motueka (Lat -41.1117; Long 173.0170). The site is located in the middle of a residential area, as shown in Figure 2.1.

The authors have been provided with information about the monitoring site and informed of the typical activities in the surrounding areas that may contribute to particulate matter concentrations. These details informed the conceptual receptor model described in Section 2.5.

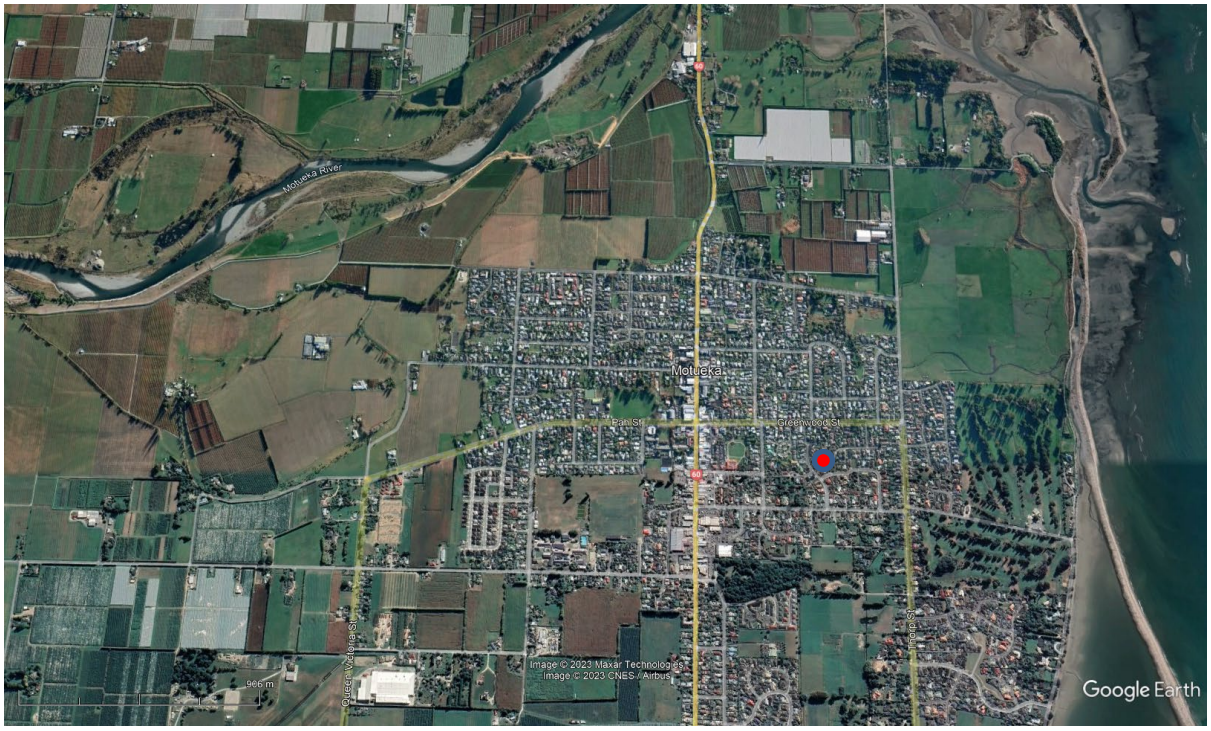

Figure 2.1 Location of Motueka $PM_{2.5}$ monitoring site (●). Source: Google Earth, 2023.

The area immediately around the site is flat and predominately residential, with local urban road traffic. The coast (Tasman Bay) is approximately 1 km directly east, and further residential properties lie to the north and northwest. West of the site, approximately 0.5 km away, is State Highway 60, which runs through the main commercial precinct of Motueka where a variety of commercial, light industrial and engineering activities are located. Land use surrounding Motueka is predominantly agricultural, with the Motueka River to the northwest.

2.2 Description of Particulate Matter Sampling

Particulate matter samples (24-hour) for analysis were collected onto PTFE for $PM_{2.5}$ (Whatman PTFE membrane, 47 mm, 0.4 µm) at the site using a Partisol gravimetric air-quality sampler (Thermo Scientific 2025i). A total of 327 samples (plus field and lab blanks) were collected on a daily sampling regime over this period. It is noted that there were six periods of no data captured due to various mechanical issues, including pump failure and shuttle errors, and noise complaints. Three of these gaps were during the winter months, so there is an incomplete dataset over the winter period. All particulate matter sampling and some systems maintenance at the air-quality monitoring site was carried out by TDC, and as such,

TDC maintains all records of equipment, flow rates and sampling methodologies used for the sampling regime. Watercare Laboratory Services was contracted to undertake some of the ambient air-quality equipment maintenance. Filter conditioning, weighing and re-weighing for particulate matter gravimetric mass determinations were also carried out by Watercare Laboratory Services. Mass concentrations of particulate matter were determined gravimetrically, where a filter of known weight was used to collect the samples from a known volume of sampled air. The loaded filters were then re-weighed to obtain the mass of collected particulate matter. The average particulate matter concentration in the volume of air sampled was then calculated.

2.3 Receptor Modelling Process

The multi-variate analysis of air particulate matter sample composition (also known as receptor modelling) provides groupings (or factors) of elements that vary together over time. This technique effectively 'fingerprints' the sources that are contributing to airborne particulate matter and the mass of each element (and the particulate matter mass) attributed to that source. In this study, the primary source contributors were determined using results from the Positive Matrix Factorisation (PMF analysis) of the particulate matter elemental composition.

A critical point for understanding the receptor modelling process is that the PMF model can produce any number of solutions, all of which may be mathematically correct (Paatero et al. 2002). The 'best' solution (e.g. number of factors, etc.) is generally determined by the practitioner after considering the model diagnostics and a review of the available factor profiles and contributions (to check physical interpretability). Most commonly used receptor models are based on conservation of mass from the point of emission to the point of sampling and measurement (Hopke 1999). Their mathematical formulations express ambient chemical concentrations as the sum of products of species abundances in source emissions and source contributions. In other words, the chemical profile measured at a monitoring station is resolved mathematically to be the sum of a number of different factors or sources. As with most modelling approaches, receptor models based on the conservation of mass are simplifications of reality and have the following general assumptions:

1. Compositions of source emissions are constant over the period of ambient and source sampling.
2. Chemical species do not react with each other (i.e. they add linearly).
3. All sources with a potential for contributing to the receptor have been identified and had their emissions characterised.
4. The number of sources or source categories is less than or equal to the number of species measured.
5. The source profiles are linearly independent of each other.
6. Measurement uncertainties are random, uncorrelated and normally distributed.

The effects of deviations from these assumptions are testable and can therefore allow the accuracy of source quantification to be evaluated. Uncertainties in input data can also be propagated to evaluate the uncertainty of source contribution estimates. There are a number of natural physical restraints that must be considered when developing a model for identifying and apportioning sources of airborne particles; these are (Hopke 2003):

- the model must explain the observations
- the predicted source compositions must be non-negative

- the predicted source contributions must be non-negative, and
- the sum of predicted elemental mass contributions from each source must be less than or equal to measured mass for each element.

These constraints need to be kept in mind when conducting and interpreting any receptor modelling approach, particularly as a receptor model is still an approximation of the real-world system. Several factors also affect the nature of a sources' particle composition and its contributions to ambient loadings (Brimblecombe 1986; Hopke 1999; Seinfeld and Pandis 2006):

1. The composition of particles emitted from a source may vary over time.
2. The composition of particles is modified in the atmosphere through a multitude of processes and interactions, for example:
   - Adsorption of other species onto particle surfaces.
   - Gas to particle conversions forming secondary particulate matter, for example the conversion of SO_2 gas to SO_4^{2-}.
   - Volatilisation of particle components, such as organic compounds, or volatilisation of Cl through reaction with acidic species.
   - Interaction with and transformation by solar radiation and free radicals in the atmosphere, such as the OH and NO_3 species.

The analytical processes used in this study did not analyse for nitrate (elemental hydrogen, carbon, oxygen and nitrogen are not detectable by XRF techniques), so the missing mass that the analysis does not explain is likely a combination of nitrate and other unmeasured species, such as hydrocarbons and bound water. Measurement of the ionic components in PM_{10} at other New Zealand sites during winter indicates that aerosol nitrate species (primarily as NH_4NO_3) revealed that the nitrate content contributes approximately 0.25 µg m^{-3} in Auckland (Ancelet and Davy 2015) and 0.75 µg m^{-3} in Timaru (Scott 2014) to total particulate matter mass during winter and somewhat less during other seasons due to atmospheric processing and thermodynamic equilibria (Seinfeld and Pandis 2006). Note that nitrate aerosol, like secondary sulphate, is primarily in the $PM_{2.5}$ particle size fraction.

Analytical noise is also introduced during the species measurement process, such as analyte interferences and limits of detection for species of interest. These are at least in the order of 5% for species well above its respective detection limit and 20% or more for those species near the analytical method detection limit (Hopke 1999). Further details on data analysis and dataset preparation are provided in Appendix 1.

2.4 Data Analysis and Reporting

The receptor modelling results within this report have been produced in a manner that provides as much information as possible on the relative contributions of sources to particulate matter concentrations so that it may be used for monitoring strategies, air-quality management and policy development. The data have been analysed to provide the following outputs:

1. Masses of elemental species apportioned to each source.
2. Source elemental profiles.
3. Average particulate matter mass apportioned to each source.
4. Temporal variations in source mass contributions (time-series plots).

5. Seasonal variations in source mass contributions. For the purposes of this study, summer has been defined as December–February, autumn as March–May, winter as June–August and spring as September–November.
6. Analysis of source contributions on peak particulate matter days.

Table 2.1 presents the relevant standards, guidelines and targets for $PM_{2.5}$ concentrations.

Table 2.1 Standards, guidelines and targets for $PM_{2.5}$ concentrations.

Particle Size	Averaging Time	Ambient Air Quality Guideline	MfE* 'Acceptable' Air Quality Category	National Environmental Standard
$PM_{2.5}$	24 hours	25 µg m^{-3} (monitoring)	17 µg m^{-3}	N/A

* Ministry for the Environment air-quality categories, taken from Ministry for the Environment (1997).

2.4.1 Conditional Probability Function Analysis

A useful data analysis method is to investigate the relationship between the source contributions and wind direction. Bivariate polar plots using the source contributions to particulate matter were produced using R statistical software and the *openair* package (R Core Team 2015; Carslaw 2012; Carslaw and Ropkins 2012). Using bivariate polar plots, source contributions can be shown as a function of both wind speed and direction, providing invaluable information about potential source regions and how pollution from a specific source builds up. To produce the polar plots, wind speeds and directions were vector-averaged using functions available in *openair*. A full description of the vector averaging process can be found in Carslaw (2012).

Conditional Probability Function (CPF) analysis provides a method to find the directions for which high values of source contributions are likely to be related (Ashbaugh et al. 1985). The probability that a source contribution originates from a given wind direction is estimated by comparing the wind direction distribution for the upper 25% of source contributions relative to the total wind direction distribution.

$$CPF_{\Delta\theta} = \frac{m_{\Delta\theta}}{n_{\Delta\theta}}$$

where:

- $m_{\Delta\theta}$: number of occurrences from wind sector $\Delta\theta$ for the upper 25% of source contributions.
- $n_{\Delta\theta}$: total number of occurrences from the same wind sector.

Sources are likely to be located in the directions that have high CPF values. Because of the smoothing involved, the colour scale is only to provide an indication of overall pattern and should not be interpreted in concentration units.

2.5 Conceptual Receptor Model for Particulate Matter at Motueka

An important part of the receptor modelling process is to formulate a conceptual model of the receptor site. This means understanding and identifying the major sources that may influence ambient particulate matter concentrations at the site. For the Motueka site, the initial conceptual model includes local emission sources:

- Motor vehicles – all roads in the area act as line sources, and roads with higher traffic densities will dominate.
- Domestic activities – likely to be dominated by biomass combustion activities, such as emissions from solid fuel fires used for domestic heating during the winter.
- Industrial emissions from combustion processes (boilers) and dust-generating activities such as excavation, construction and bulk storage handling.
- Local wind-blown soil or road dust sources may also contribute.

Sources that originate further from the monitoring site would also be expected to contribute to ambient particle loadings; these include:

- Marine aerosol (sea salt) generated in the oceanic regions around New Zealand.
- Secondary particulate matter resulting from atmospheric gas-to-particle conversion processes – includes sulphates, nitrates and organic species.

Another category of emission sources that may contribute are those considered to be 'one-off' emission sources:

- Fireworks displays and other special events (e.g. Guy Fawkes Day).
- Short-term roadworks and demolition/construction activities.

The variety of sources described above can be recognised and accounted for using appropriate data analysis methods such as the application of geochemical principles, examination of seasonal differences, temporal variations and receptor modelling itself.

2.6 Local Meteorology at Motueka

A meteorological station owned and operated by TDC was located at Motueka Sports Park approximately 1 km southwest of the Ledger Goodman Park air-quality monitoring site. As shown in Figure 2.2, the predominant wind directions were from the southwesterly quadrant for the monitoring period (January 2022 – January 2023). Seasonal differences in wind speed and direction were evident, as presented in Figure 2.3. Winds were lighter and predominantly from the southwest during autumn, winter and spring, with a greater percentage of stronger northeasterly winds during summer.

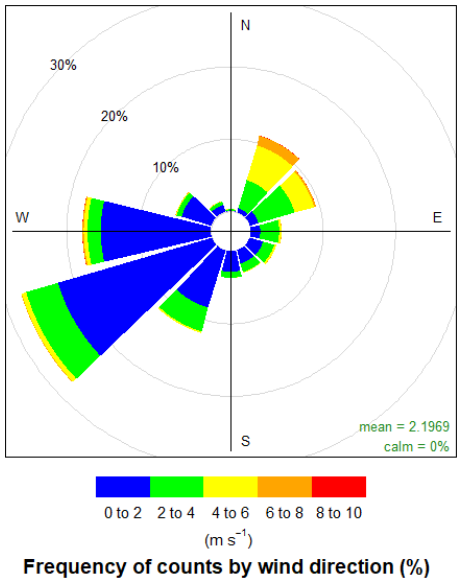

Figure 2.2 Motueka wind rose for the monitoring period (January 2022 – January 2023).

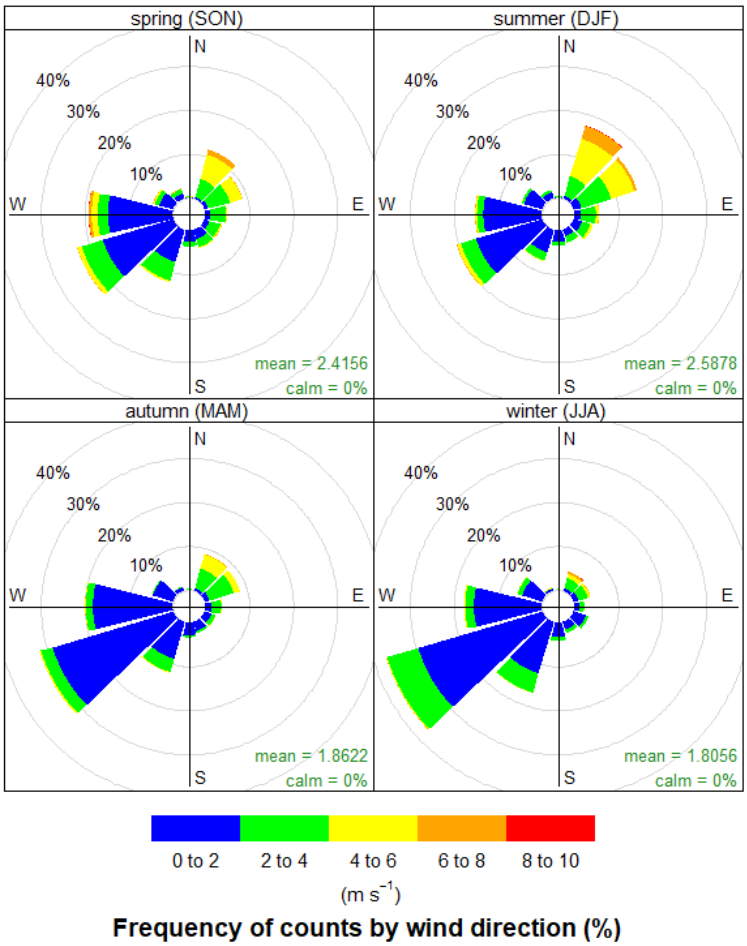

Figure 2.3 Seasonal wind roses for the monitoring period at Motueka (January 2022 – January 2023).

Mean monthly temperatures at the Motueka site were lowest during the winter period (June to August), as shown in Figure 2.4.

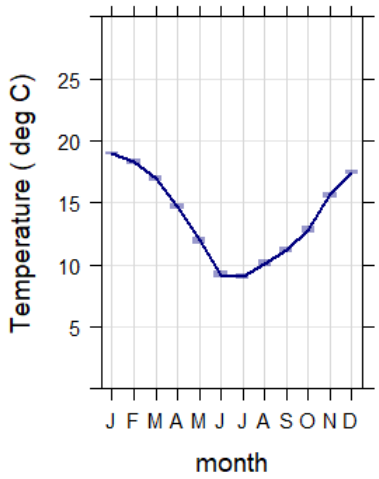

Figure 2.4 Average monthly temperature at Motueka during the monitoring period (January 2022 – January 2023). Shaded bars represent the 95% confidence intervals.

2.7 $PM_{2.5}$ Concentrations at Motueka

Mass concentrations were determined gravimetrically for the Ledger Goodman Park $PM_{2.5}$ sample filters. Figure 2.5 presents the $PM_{2.5}$ monitoring results (24-hour averages, midnight-to-midnight sampling regime) over the monitoring period (1 January 2022 – 5 January 2023).

Gaps present in Figure 2.5 are from sampler outages and/or maintenance. $PM_{2.5}$ was equal to or above the WHO guideline concentration (15 µg m^{-3} as a 24-hour average) on 26 occasions during the monitoring period. The observed winter peak in $PM_{2.5}$ concentrations at Motueka is a common occurrence in New Zealand towns and cities.

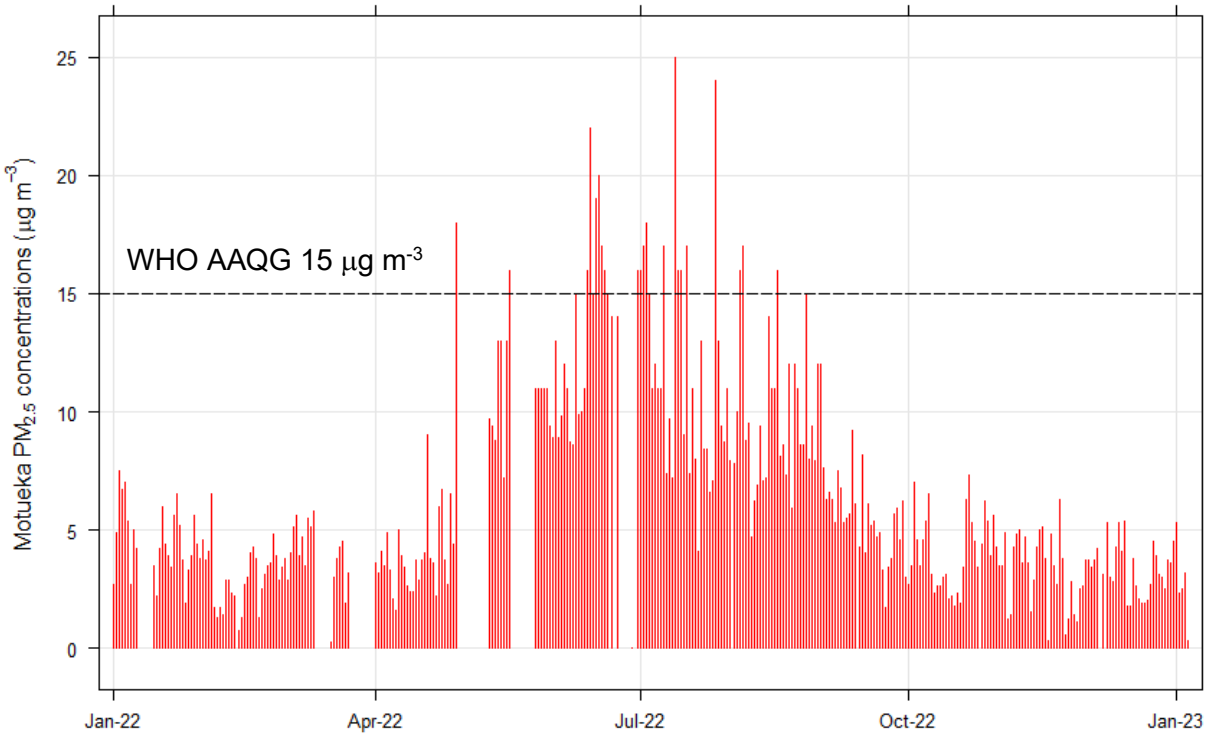

Figure 2.5 Gravimetric $PM_{2.5}$ (24-hour average) concentrations at Motueka (data supplied by TDC). Note that the gaps in the graph are due to missing samples. AAQG = Ambient Air Quality Guidelines.

Figure 2.6 shows that $PM_{2.5}$ concentrations at Motueka have a seasonal pattern, with peak concentrations occuring during winter. This pattern is likely to be explained by the types of sources contributing to $PM_{2.5}$ concentrations at the site.

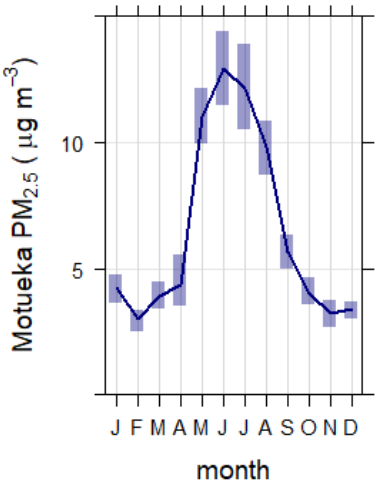

Figure 2.6 Temporal and seasonal variations in $PM_{2.5}$ (24-hour average) concentrations at Motueka. Shaded areas represent the 95% confidence intervals in the calculated mean.

3.0 RECEPTOR MODELING ANALYSIS OF PARTICULATE MATTER AT MOTUEKA

3.1 Analysis of Particulate Matter Samples Collected at Motueka

$PM_{2.5}$ samples at Motueka were collected using a Partisol gravimetric sequential sampler system, on a daily sampling regime (midnight to midnight). Overall, 327 $PM_{2.5}$ samples were collected from January 2022 to January 2023. $PM_{2.5}$ elemental and black carbon concentrations were determined using XRF and light reflection, respectively, as described in Appendix 1.

3.1.1 Composition of Particulate matter at Motueka

Elemental concentrations in the $PM_{2.5}$ samples collected at the Motueka monitoring site are presented in Table 3.1. The data shows that $PM_{2.5}$ concentrations are dominated by black carbon, with peak concentrations during the winter months. Other important elemental constituents included K, Na, Cl, Si, Al, S and Fe, indicating that combustion sources, marine aerosol, crustal matter and secondary sulphate particles were likely to be important contributors to $PM_{2.5}$ concentrations at the monitoring site. Some measured species were close to or below their respective limit of detection (LOD) in each of the samples. Elemental correlation plots are provided in Figure A2.2 in Appendix 2.

Table 3.1 Elemental concentrations in $PM_{2.5}$ samples from Motueka (327 samples). BC = black carbon.

	Unit	Average	Maximum	Minimum	Median	Std. Dev.	Average LOD	% > LOD
$PM_{2.5}$	µg m-3	6	25	0	5	4	-	-
BC	ng m-3	1380	6375	0	566	1502	105	87
Na	ng m-3	261	1232	0	181	229	6	99
Mg	ng m-3	29	151	0	20	28	46	24
Al	ng m-3	26	198	0	21	27	15	65
Si	ng m-3	42	401	0	26	56	6	92
P	ng m-3	0	7	0	0	1	1	7
S	ng m-3	110	444	0	87	82	21	95
Cl	ng m-3	350	2125	0	216	368	2	98
K	ng m-3	84	319	0	64	63	2	99
Ca	ng m-3	11	66	0	8	13	9	46
Ti	ng m-3	2	16	0	1	2	1	49
V	ng m-3	0	1	0	0	0	0	10
Cr	ng m-3	0	2	0	0	0	1	1
Mn	ng m-3	1	6	0	0	1	2	25
Fe	ng m-3	13	84	0	9	12	2	91
Co	ng m-3	19	584	0	0	102	0	23
Ni	ng m-3	0	4	0	0	0	1	13
Cu	ng m-3	1	20	0	1	2	2	19

	Unit	Average	Maximum	Minimum	Median	Std. Dev.	Average LOD	% > LOD
Zn	ng m-3	3	32	0	2	4	1	71
Ga	ng m-3	1	3	0	0	1	1	21
As	ng m-3	1	17	0	0	3	1	21
Se	ng m-3	0	5	0	0	1	2	7
Br	ng m-3	9	2414	0	2	133	1	63
Sr	ng m-3	1	5	0	0	1	2	19
Mo	ng m-3	1	9	0	0	1	2	16
Cd	ng m-3	8	42	0	5	10	18	18
Sn	ng m-3	4	23	0	1	5	6	24
Sb	ng m-3	4	29	0	1	5	10	13
Te	ng m-3	6	29	0	4	6	9	29
Cs	ng m-3	10	51	0	5	12	18	24
Ba	ng m-3	8	52	0	2	11	20	14
La	ng m-3	11	71	0	1	15	28	14
Ce	ng m-3	52	352	0	3	73	144	13
Sm	ng m-3	35	324	0	0	58	99	13
Pb	ng m-3	3	20	0	2	3	3	36
Hg	ng m-3	1	11	0	0	2	1	19
In	ng m-3	3	23	0	0	4	5	19
W	ng m-3	104	748	0	4	149	285	13

Of the measured heavy metals, both arsenic (As) and lead (Pb) were observed to also have peak winter concentrations, as presented in Figure 3.1.

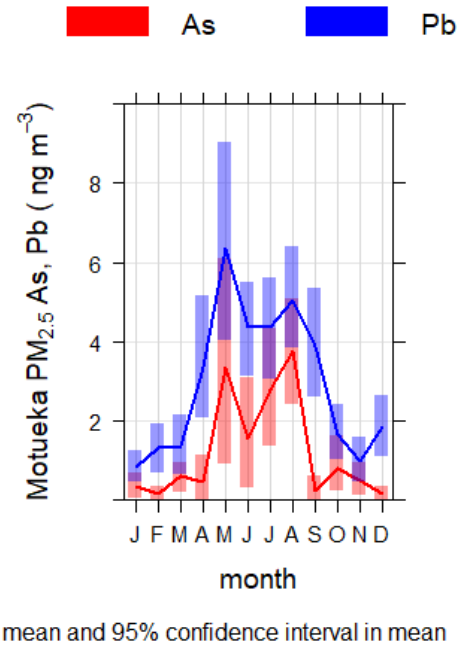

Figure 3.1 Monthly average elemental concentrations for As in $PM_{2.5}$ samples from Motueka.

Neither As (annual average = 1.2 ng m^{-3}) nor Pb (three-month rolling average = 4 ng m^{-3}) exceeded the Ambient Air Quality Guidelines (5.5 ng m^{-3} and 200 ng m^{-3}, respectively). However, inhalation of such contaminated air particulate matter has been shown to result in biological uptake in humans, with the long-term effects of exposure as yet unknown (Dirks et al. 2020).

3.2 Source Contributions to Particulate Matter at Motueka

The $PM_{2.5}$ compositional data were analysed to provide information on contributing sources using PMF with multiple re-iterations such that that robust solutions and source attributions were arrived at. Sources of particulate matter emissions or generation include particles across the size-range spectrum and therefore contribute to both fine and coarse size fractions, although some source types will contribute more to one size fraction than the other. For example, combustion sources such as domestic solid fuel fires or motor vehicle tailpipe emissions produce particles in the sub-micron size range and are therefore largely confined to the $PM_{2.5}$ fraction. Windblown dust; road dust generated by the turbulent passage of motor vehicles over local roads; sea salt; or industrial processes that involve mechanical grinding, sorting, storage and transport of bulk materials predominantly produce particles in the larger size ranges (greater than $PM_{2.5}$), although some 'tail' of particle sizes does extend down into the $PM_{2.5}$ size fraction.

3.2.1 Sources of $PM_{2.5}$ at Motueka

Five source types were identified from PMF receptor modelling analysis of the Motueka $PM_{2.5}$ elemental data. Table 3.2 and Figure 3.2 present the source elemental profiles and $PM_{2.5}$ contributions extracted from the PMF analysis. The source contributors identified were found to explain 96% of the $PM_{2.5}$ mass on average.

The sources identified were:

- **Biomass combustion:** The first factor was identified as biomass combustion based on the dominance of black carbon and K in the profile (Fine et al. 2001; Khalil and Rasmussen 2003). Trace amounts of As and Pb were also strongly associated with the biomass combustion profile. This phenomenon is consistent throughout New Zealand and indicates co-combustion of copper-chrome-arsenate-treated (CCA) timber and old painted timber, respectively (Davy et al. 2014).
- **Motor vehicles:** The second factor was identified as motor vehicles because of the presence of black carbon, Fe, Cu and Zn as significant elemental components. This profile is likely a combination of tailpipe (black carbon and Zn from fuel combustion) and re-entrained road dust emissions (Al, Si, Ca, Fe crustal matter components; Cu from brake dust);
- **Secondary sulphate:** The third factor was identified as sulphate because of the dominance of sulphur in the profile. This source contribution was likely to be from secondary sulphate aerosol produced in the atmosphere from gaseous precursors.
- **Marine aerosol:** The fourth factor was identified as a marine aerosol source because of the predominance of Na and Cl, along with some Mg, S, K and Ca.
- **Soil:** The fifth source has been identified as originating from activities that generate crustal matter, as the chemical profile is dominated by elemental aluminium and silicon typical of the bulk composition of the earth's crust.

Further analysis of the $PM_{2.5}$ source contributors is provided in the following sections.

Table 3.2 Average source elemental concentration profiles for $PM_{2.5}$ samples from Motueka (based on 327 samples). BC = black carbon.

	Biomass Combustion (ng m^{-3})	Motor Vehicles (ng m^{-3})	Secondary Sulphate (ng m^{-3})	Marine Aerosol (ng m^{-3})	Soil (ng m^{-3})
$PM_{2.5}$	3750	350	530	860	390
BC	1237.1	67.5	29.3	39.7	1.7
Na	15.1	0.16	48.7	183.3	13.1
Mg	1.2	0.1	4.3	19.5	3.3
Al	2.2	1.9	2.4	7.7	11.6
Si	1.3	3.9	3.1	4.7	29.6
S	10.8	1.3	59.8	27.5	8.1
Cl	27.3	0.0	9.9	297.9	11.7
K	55.9	4.3	7.5	9.6	4.3
Ca	0.0	1.8	1.5	4.5	2.8
Ti	0.1	0.1	0.0	0.1	1.1
Fe	1.0	6.2	0.4	0.5	4.3
Cu	0.2	0.2	0.1	0.1	0.0
Zn	1.8	0.5	0.1	0.2	0.0
As	1.0	0.0	0.0	0.0	0.0
Pb	1.5	0.3	0.1	0.0	0.0

Table 3.2 also shows that biomass combustion is the dominant contributing source to average $PM_{2.5}$ concentrations at Motueka. Note that the summation of elemental components does not equal particulate matter mass, as this analysis was not for compounds (which includes oxides and other unmeasured species as described in Section 2.1) but for proportional elemental co-variance and the proportion of particulate matter mass that is also co-variant with those elemental species.

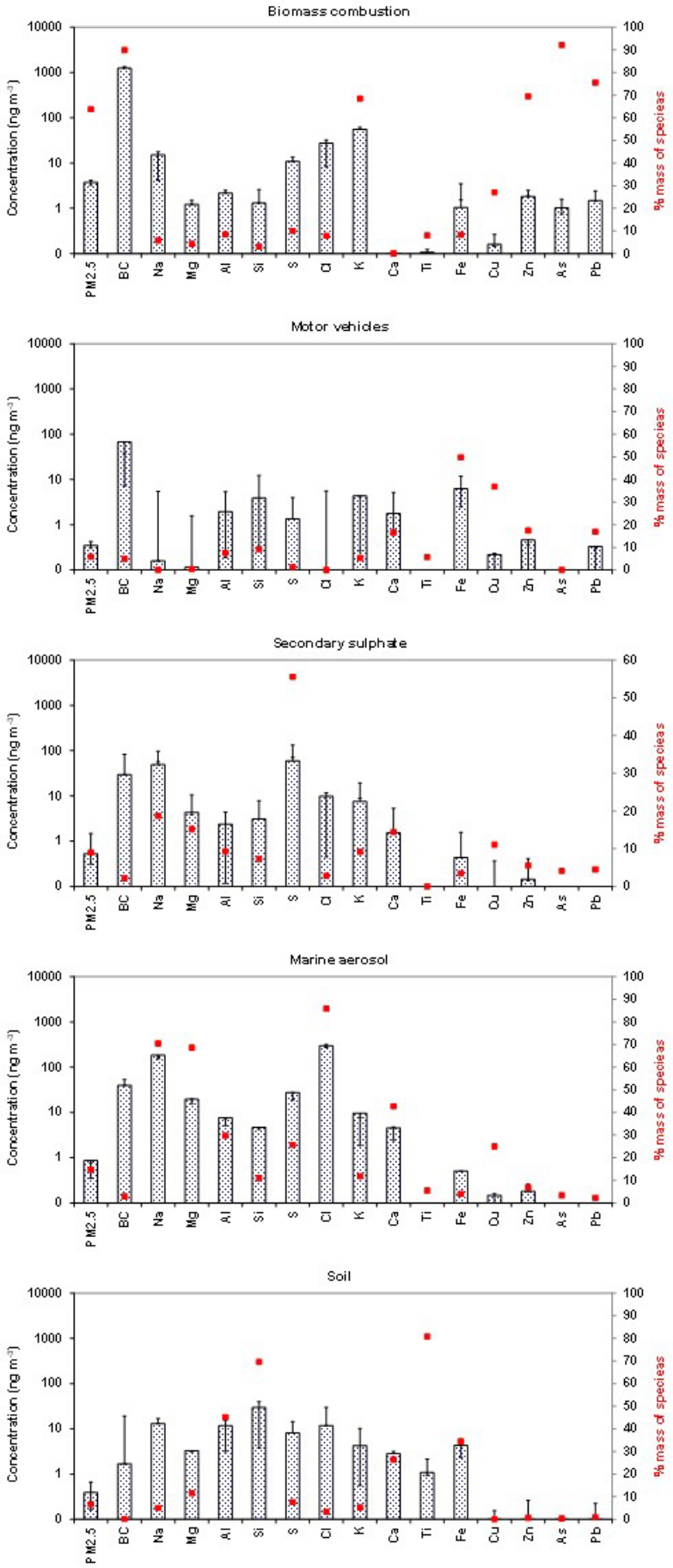

Figure 3.2 Source elemental concentration profiles for $PM_{2.5}$ samples from Motueka. The red dots represent the percentage of each chemical species attributed to each source.

Figure 3.3 presents the relative source contributions to $PM_{2.5}$ in Motueka. Also included in this figure are the 5th and 95th percentile confidence limits (bottom and top of error bar, respectively) in average mass contributions attributed to each of the sources, indicating the variability in average mass contributions over the monitoring period.

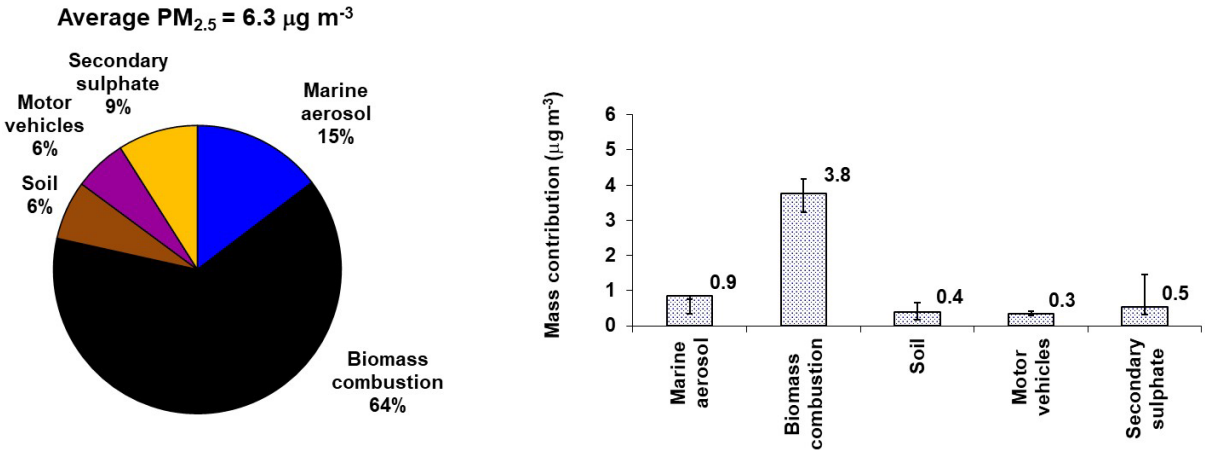

Figure 3.3 Average source mass contributions to $PM_{2.5}$ at Motueka over the monitoring period.

The average $PM_{2.5}$ source contributions over the entire monitoring period estimated from the PMF analysis showed that biomass combustion (64%) was the most significant contributor to $PM_{2.5}$ mass, with marine aerosol (15%) and secondary sulphate (9%) the next highest, while motor vehicles (6%) and soil (6%) had the lowest contributions to $PM_{2.5}$ mass.

3.3 Temporal Variations in Source Contributions to Particulate Matter at Motueka

Temporal variations in the source contributions to $PM_{2.5}$ at Motueka are presented in Figure 3.4. It was evident that airborne particulate matter mass is dominated by the biomass combustion source during winter, which arises primarily from emissions from solid fuel fires used for domestic heating. During other time periods, marine aerosol, secondary sulphate and crustal matter contributions can be significant. The motor-vehicle source contributed low levels of $PM_{2.5}$ during the monitoring period, most likely due to the local level of traffic activity near the Motueka monitoring site.

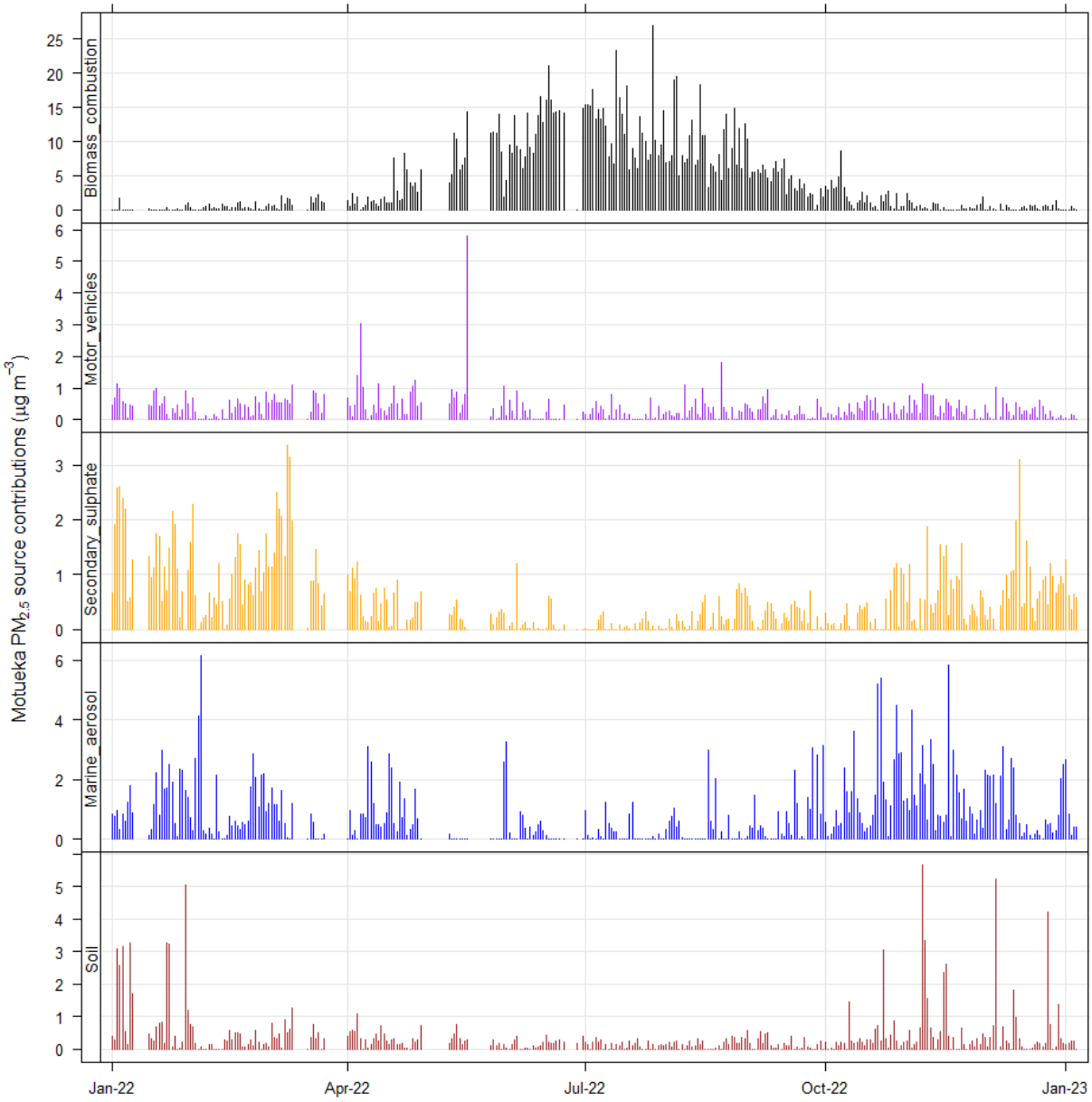

Figure 3.4 Temporal variations in relative source contributions to $PM_{2.5}$ mass (24-hour average) at the Motueka site.

3.3.1 Seasonal Variations in Particulate Matter Sources at Motueka

Examining the seasonal patterns in source contributions is useful for identifying sources and understanding the time of year when they may have the most impact on particulate matter concentrations. Figure 3.5 presents the temporal variation in average monthly source contributions to $PM_{2.5}$ concentrations at the Motueka site and shows that there was a distinctive seasonal pattern in contribution to $PM_{2.5}$ concentrations for some sources.

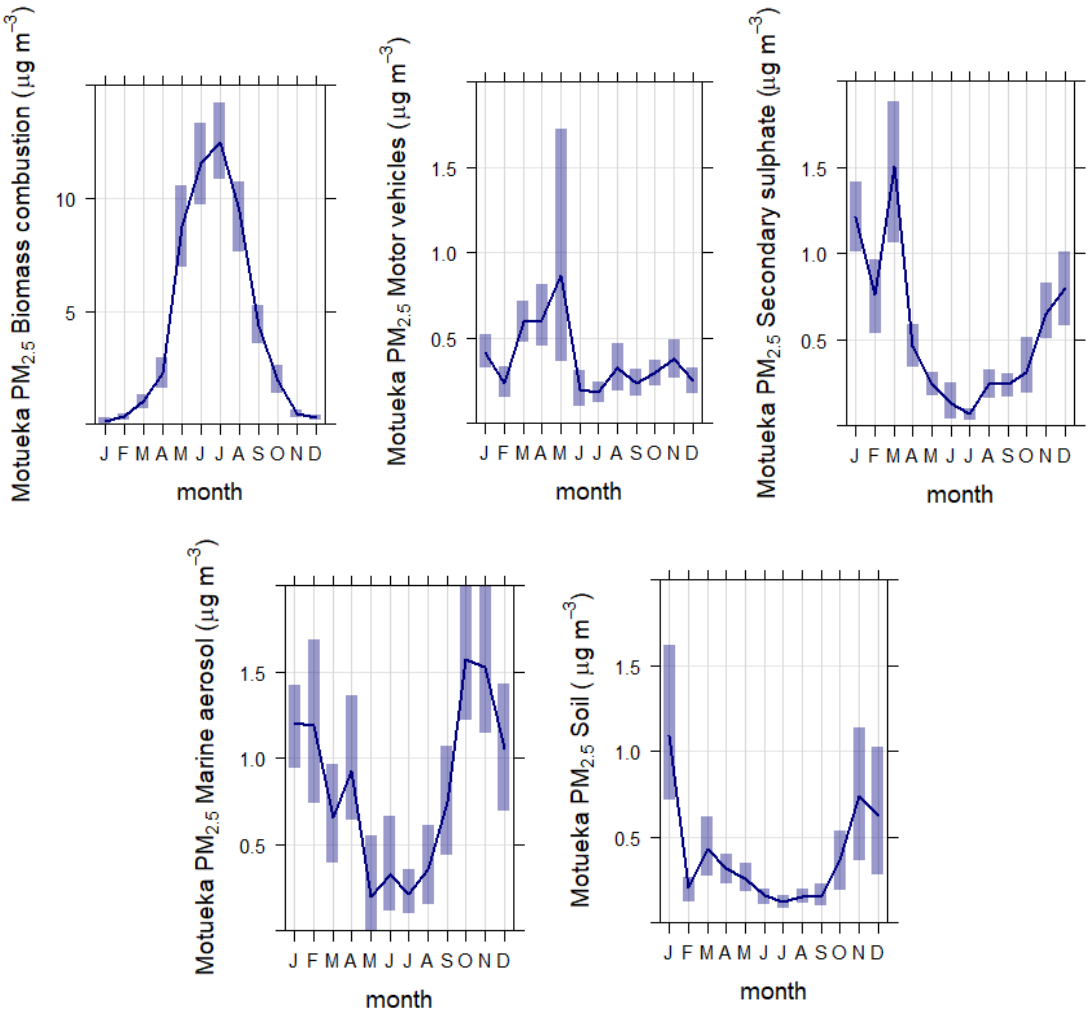

Figure 3.5 Average monthly source contributions to $PM_{2.5}$ concentrations at Motueka. Shaded bars represent the 95% confidence intervals in the calculated mean.

The dominant source of $PM_{2.5}$ at Motueka was biomass combustion, which had a distinct winter peak due to the association of this source with solid fuel fire (wood burner) emissions for domestic space heating. The motor vehicle source did not demonstrate any distinctive seasonality. Significant sources of secondary sulphate include combustion emissions from high sulphur fuels (for example, coal and ships using residual oil), industrial emissions of precursor gases, marine phytoplankton activity (release of dimethyl sulphide as a gaseous precursor) and volcanic emissions. A similar seasonality in secondary sulphate concentrations has been observed at other monitoring sites in New Zealand (Davy and Trompetter 2018). The marine aerosol (sea salt) source concentrations were generally lower in winter but were likely to be primarily a meteorologically generated source (wind field strength over oceanic fetch) (Fitzgerald 1991). A peak in marine aerosol during spring (October, November) is typical for New Zealand locations and a reflection of strong equinox winds over the Southern Ocean. The crustal matter source (soil) shows that peak concentrations occur during the summer months and may be associated with agricultural activities (ploughing/harvesting) in the surrounding countryside.

A feature of the monthly source-contribution plots presented in Figure 3.5 is the variability in day-to-day source contributions that give rise to the uncertainty in the mean estimate, as indicated by the 95 percentile confidence intervals (shaded bars on the line plots). This is likely to be the result of variable source activity coupled with meteorological influences (particulate matter emissions from mono-directional sources will only be carried to the monitoring site when the wind is blowing in the right direction).

3.3.2 Daily Variations in Particulate Matter Sources at Motueka

Source contributions to particulate matter concentrations were analysed by day of the week to investigate any potential weekday/weekend variations. Analysis of source contributions to particulate matter concentrations show that the $PM_{2.5}$ motor-vehicle source contributions were lower on weekends than weekdays (statistically significant at the 95% confidence intervals), as presented in Figure 3.6, and is likely to be indicative of lower traffic densities during the weekend than weekdays, associated with normal working week and commercial activity.

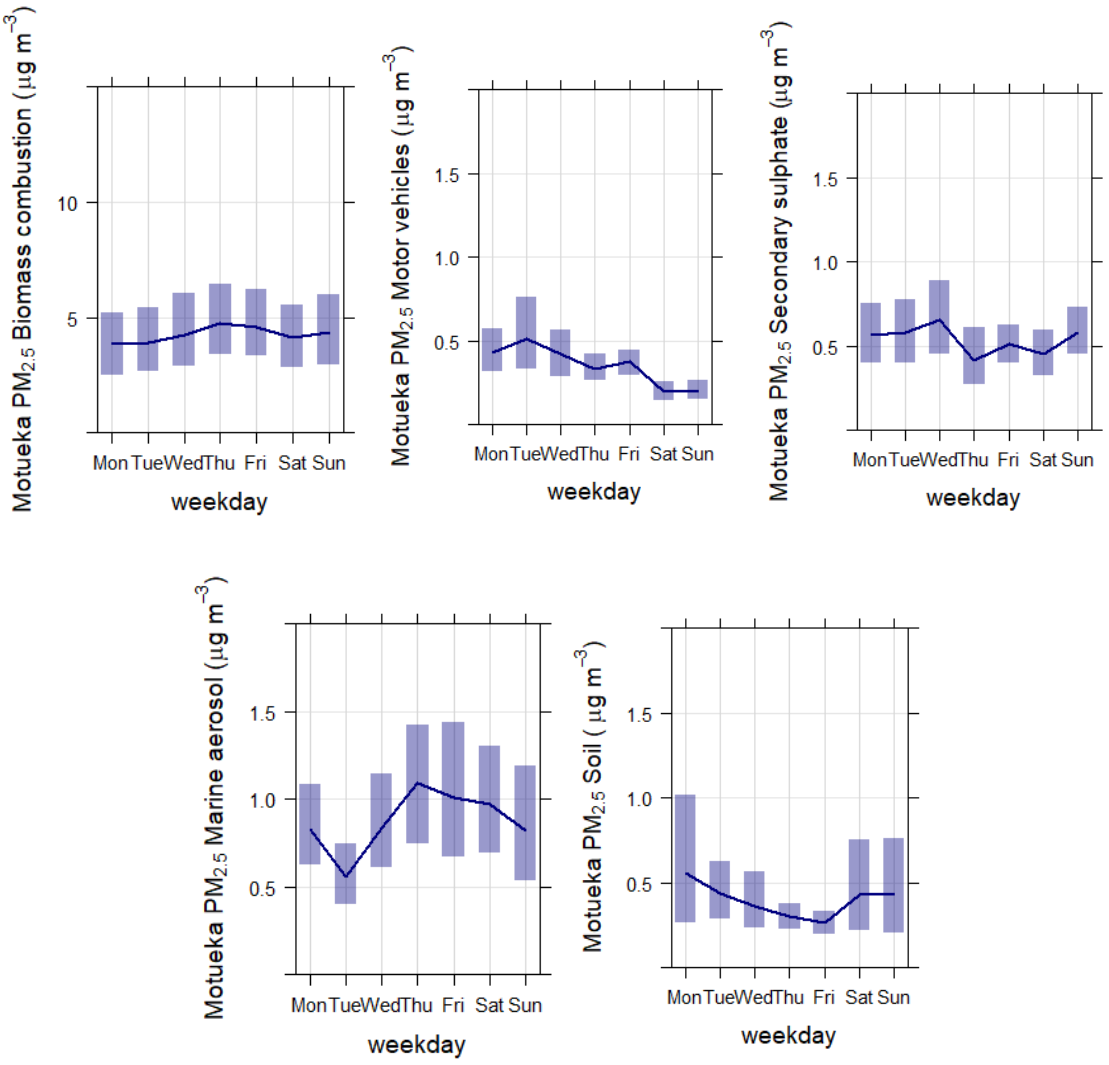

Figure 3.6 Variation in source contributions to $PM_{2.5}$ at Motueka by day of the week. Shaded bars represent the 95% confidence intervals.

3.4 Variations in $PM_{2.5}$ Source Contributions at Motueka with Wind Direction

Bivariate polar plots using the source contributions to $PM_{2.5}$ were produced using R statistical software and the *openair* package (R Core Team 2015; Carslaw 2012; Carslaw and Ropkins 2012). Using bivariate polar plots, source contributions can be shown as a function of both wind speed and direction, providing invaluable information about potential source regions and how pollution from a specific source builds up. To produce the polar plots, wind speeds and directions were vector-averaged using functions available in *openair*. A full description of the vector-averaging process can be found in Carslaw (2012). The conditional probability function statistic = 'cpf' has been used here, as described in Section 2.4.1. Because of the smoothing involved, the colour scale is only to provide an indication of overall pattern and should not be interpreted in concentration units. The meteorological data used for the polar plot analysis was that supplied by TDC from their Motueka monitoring site.

3.4.1 Biomass Combustion

Biomass combustion source contributions to $PM_{2.5}$ were primarily from domestic solid fuel fire emissions. Figure 3.7 presents a bivariate polar plot of biomass combustion contributions to $PM_{2.5}$. Figure 3.7 shows that peak biomass combustion contributions occurred under light winds (less than 2 m/s) from the southwest. This suggests that katabatic (downslope) flows under cold and calm anti-cyclonic synoptic meteorological conditions, coupled with domestic fire emissions and poor dispersion, were likely responsible for elevated particulate matter concentrations, similar to previous results in other New Zealand locations (Trompetter et al. 2010; Ancelet et al. 2012; Grange et al. 2013).

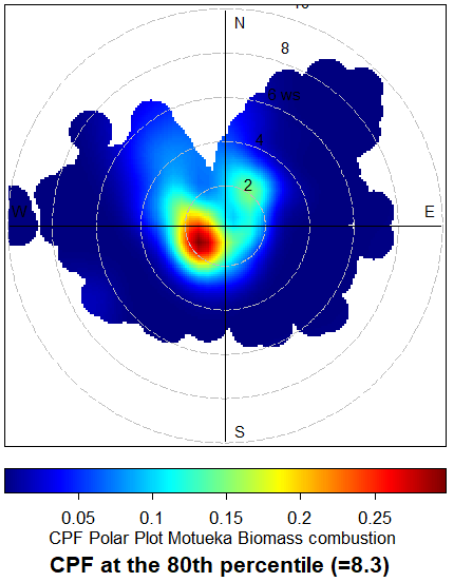

Figure 3.7 Polar plot of biomass combustion contributions to $PM_{2.5}$ concentrations. The radial dimensions indicate the wind speed in 2 m s^{-1} increments, and the colour contours indicate the relative contribution to each wind direction/speed bin.

3.4.2 Motor Vehicles

Peak motor-vehicle contributions at the monitoring site occurred under winds from the west to northwest quadrant (Figure 3.8). This is likely to represent the contribution from motor vehicles on the busiest local roads, such as High Street (State Highway 60), coupled with wind direction carrying emissions from traffic across the monitoring site. When wind direction aligns with

the centreline of roadways, the road acts as a line source, and this will convey the highest concentrations of motor vehicle emissions.

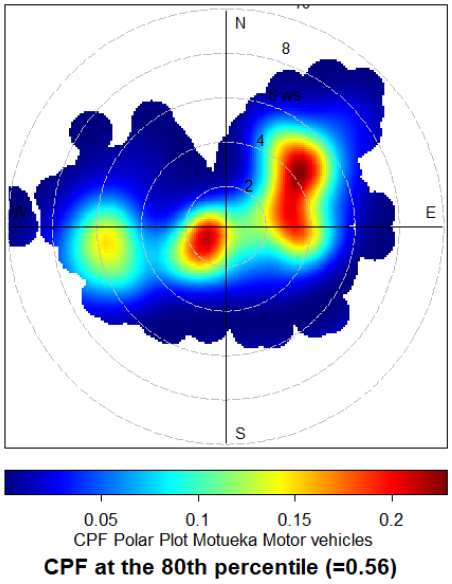

Figure 3.8 Polar plot of motor-vehicle contributions to $PM_{2.5}$ concentrations. The radial dimensions indicate the wind speed in 2 m s^{-1} increments, and the colour contours indicate the relative contribution to each wind direction/speed bin.

3.4.3 Secondary Sulphate

Peak secondary sulphate contributions at Motueka originated from northeast of the monitoring site (Figure 3.9). Sources of secondary sulphate precursor gases include the combustion of sulphur containing fuels, natural oceanic emissions (marine phytoplankton), volcanic activity and industrial emissions.

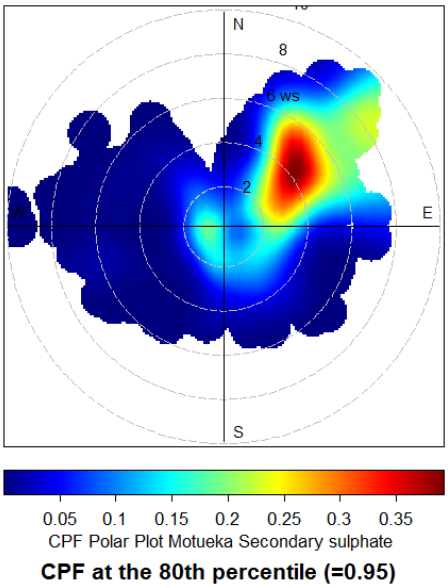

Figure 3.9 Polar plot of secondary sulphate contributions to $PM_{2.5}$ concentrations. The radial dimensions indicate the wind speed in 2 m s^{-1} increments, and the colour contours indicate the relative contribution to each wind direction/speed bin.

3.4.4 Marine Aerosol

Marine aerosol contributions in Motueka peaked under higher wind speeds from the northeast sector (Figure 3.10). The most likely source of marine aerosol was the Tasman Sea and Southern Ocean.

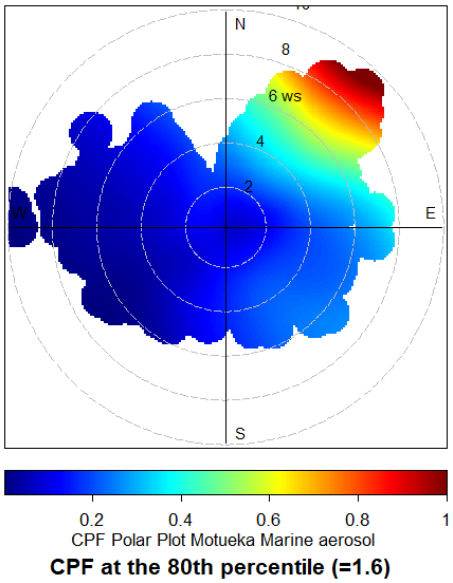

Figure 3.10 Polar plot of marine aerosol contributions to $PM_{2.5}$, concentrations. The radial dimensions indicate the wind speed in 2 m s^{-1} increments, and the colour contours indicate the relative contribution to each wind direction/speed bin.

3.4.5 Soil

Figure 3.11 shows that the $PM_{2.5}$ crustal matter contributions peaked under moderate wind speeds from the northeast. The crustal matter in urban areas is likely to be generated by a combination of vehicle dusts from road surfaces, unsealed yards or other dust-generating activities such as agriculture, bulk aggregate processing, handling, storage and excavations. However, the patterns observed for the Motueka site (Figures 3.4 and 3.11) suggest that the source of crustal matter may be associated with windblown dust from the nearby coastal area.

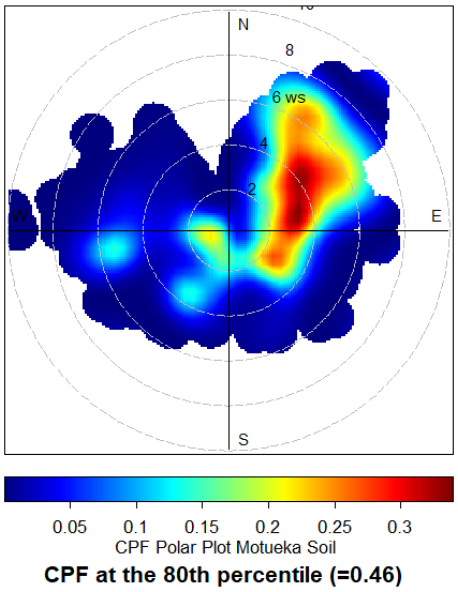

Figure 3.11 Polar plot of soil contributions to $PM_{2.5}$ concentrations. The radial dimensions indicate the wind speed in 2 m s^{-1} increments, and the colour contours indicate the relative contribution to each wind direction/speed bin.

4.0 DISCUSSION OF THE RECEPTOR MODELLING RESULTS

Monitoring of air particulate matter in Motueka showed that peak $PM_{2.5}$ concentrations occurred during winter. Five source contributors to particulate matter concentrations were identified from receptor modelling. The receptor modelling analysis showed that some source contributors had distinct seasonality and that the peak winter particulate matter concentrations were primarily influenced by biomass combustion sources.

4.1 Sources of Particulate Matter at Motueka

4.1.1 Biomass Combustion

Analysis of temporal and seasonal patterns showed that particulate matter from biomass combustion peaked during the winter (Figure 3.5) and showed no variation between days of the week (Figure 3.6). The lack of variation between days of the week was not surprising, as peak biomass combustion contributions occur under meteorological conditions conducive to the build-up of pollutants (cold and calm, anti-cyclonic conditions), which could occur on any day of the week. The biomass combustion source was most likely to have originated from domestic wood combustion for home heating and included traces of As and Pb in the source chemical profile, suggesting that CCA-treated wood and old painted timber was being used as fuel. The use of such contaminated timber as fuel for domestic fires appears to be common throughout New Zealand (Davy and Trompetter 2018).

Figure 4.1 presents the biomass combustion contribution to $PM_{2.5}$ (top), along with As and Pb concentrations measured in $PM_{2.5}$ (bottom), showing that biomass combustion contribution to $PM_{2.5}$ is present on a daily basis during the winter, while As and Pb concentrations are more variable and intermittent. This is likely due to the fact that, rather than being used as a constant percentage of solid fuels, contaminated-timber use is more opportunistic and probably only carried out by certain households in the area. This is illustrated by the scatterplot of biomass combustion contributions versus As concentrations presented in Figure 4.2, which shows that, while As concentrations tend to be higher on days with a greater contribution to $PM_{2.5}$ from the biomass combustion source, there are many occasions where As was not detected, even though biomass combustion contributions were relatively high (>5 μg m^{-3}).

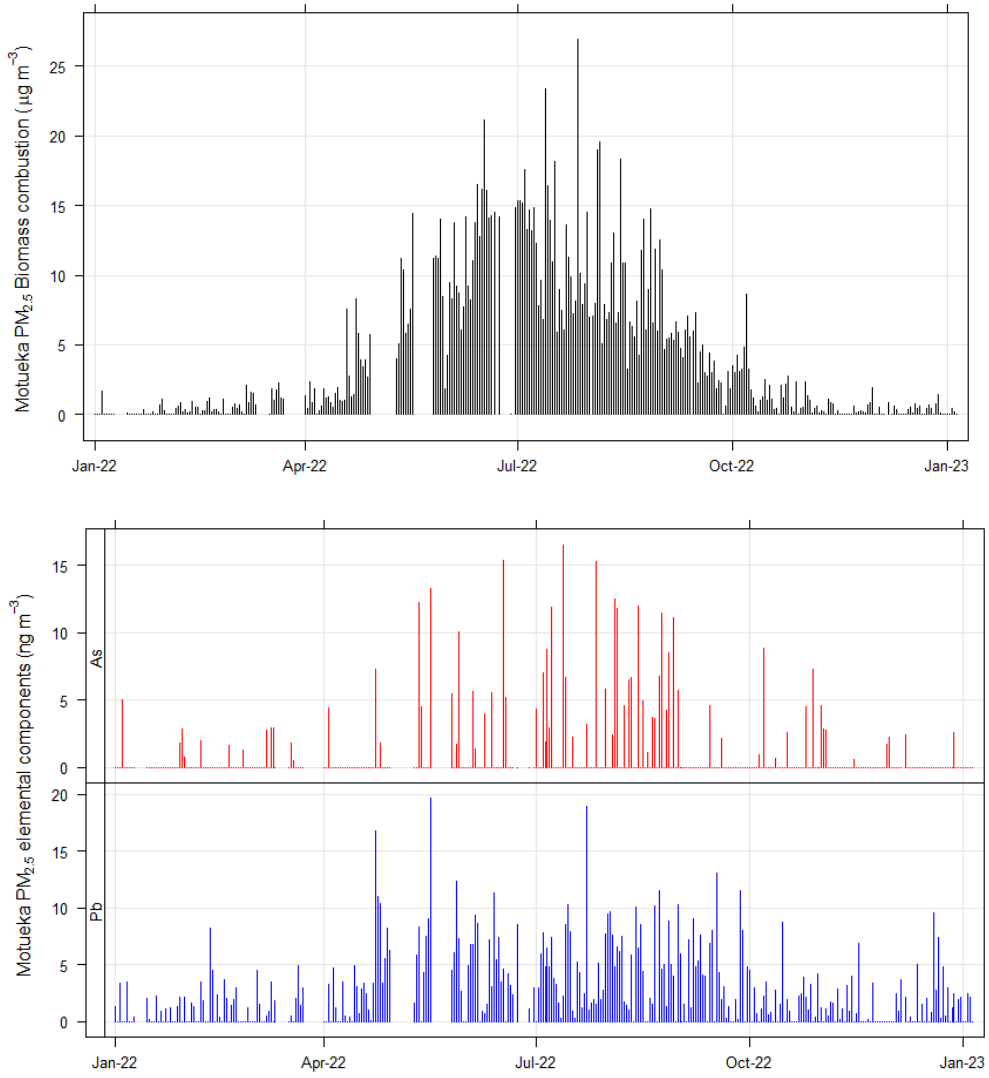

Figure 4.1 Biomass combustion contribution to $PM_{2.5}$ (top) and As and Pb concentrations measured in $PM_{2.5}$ (bottom).

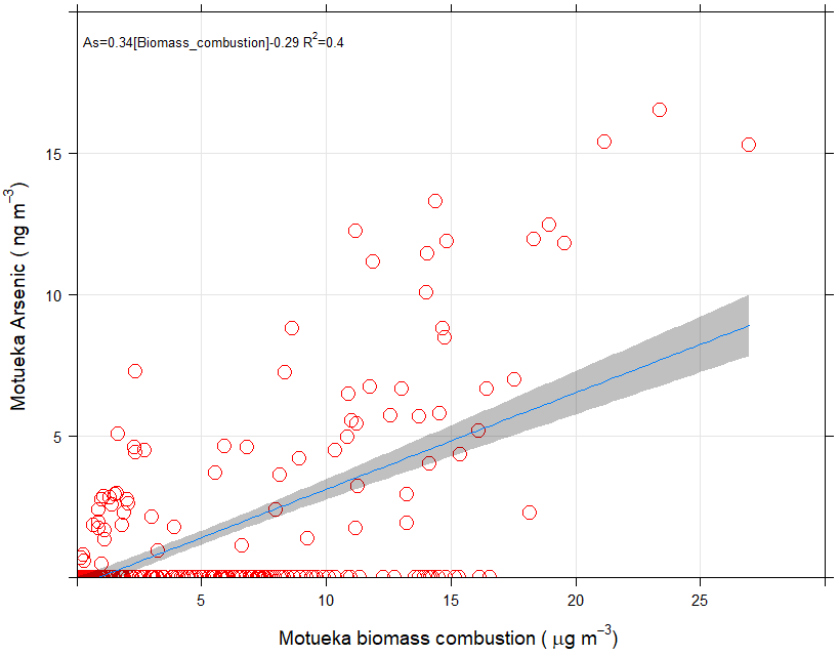

Figure 4.2 Scatterplot of biomass combustion contributions versus As concentrations.

4.1.2 Motor Vehicles

The motor-vehicle source was identified as a minor contributor to $PM_{2.5}$ (6%). As indicated in the previous sections, the motor-vehicle source is likely to be a combination of vehicular tailpipe emissions (fine particles) and re-suspended soil generated by the turbulent passage of vehicles on roads, carparking areas and unsealed yards (coarse particles).

Further support for the anthropogenic origin of the motor-vehicle source was that weekday contributions appeared to be higher than for weekends (see Figure 3.6), indicating an association with anthropogenic activity (traffic density and associated weekday commuter and commercial activities). The bivariate polar plot (Figure 3.8) for the variation of motor vehicle contributions with wind speed and direction showed that peak concentrations occurred under winds from the southwest and northeast, probably associated with traffic on nearby roads.

4.1.3 Secondary Sulphate

As presented in Figure 3.5, the secondary sulphate particulate matter source showed a strong seasonal pattern, with the highest concentrations during summer months. Analysis of the sulphate source contributions using a polar plot (Figure 3.9) showed that the secondary sulphate was transported from northeast of the sampling site. Significant sources of secondary sulphate include combustion emissions from high sulphur fuels (for example, coal and ships using residual oil), industrial emissions of precursor gases, marine phytoplankton activity (release of dimethyl sulphide as a gaseous precursor) and volcanic emissions. The atmospheric reaction pathway for these gases is similar no matter the source and, ultimately, the sulphate aerosol has a similar chemical signature that is resolved as a single source by factor analysis techniques such as PMF. Note that the conversion of precursor gases to sulphate particles can take hours to days depending on atmospheric conditions (temperature, relative humidity, solar insolation) and the presence (or absence) of other reactive species. The higher concentrations during summer are likely due to the influence of solar forcing of atmospheric chemistry and cycles in natural source (marine phytoplankton) production and/or higher shipping activity.

4.1.4 Marine Aerosol

Marine aerosol was found to be a significant contributor to $PM_{2.5}$ in Motueka at times and is generally a significant particle source in New Zealand airsheds. The elemental composition for the marine aerosol source closely resembled that of seawater, and the source profile is dominated by chlorine and sodium. Analysis of temporal and seasonal variations in marine aerosol showed higher concentrations during spring and summer, but marine aerosol concentrations could also peak at other times since the generation of marine aerosol is dependent on meteorological factors, such as wind speeds across an oceanic fetch and evaporation potential. Analysis of peak marine aerosol contributions to particulate matter concentrations (Figure 3.10) showed a distinct northeasterly directionality during higher wind speeds at Motueka and was therefore consistent with the most significant oceanic wind directions.

4.1.5 Soil

The chemical composition profile for the soil source contains aluminium and silicon as major constituents, typical of crustal matter. The soil source CPF analysis (Figure 3.11) demonstrated a strong northeasterly directionality. While local soil disturbance activities such as excavations or land clearance during the monitoring period could have been a factor, the exposed coastal area to the northeast of the site may have been the predominant source.

4.2 Analysis of Contributions to Particulate matter on Peak Days

For air-quality management purposes, contributions from the various sources to peak $PM_{2.5}$ events are of most interest. Of the days when samples were collected during the monitoring period, there were 26 days (all during winter) when $PM_{2.5}$ concentrations were equal to or higher than 15 µg m^{-3}, the WHO ambient air-quality guideline for $PM_{2.5}$. The relative source contributions to $PM_{2.5}$ on those peak days are presented in Figure 4.3.

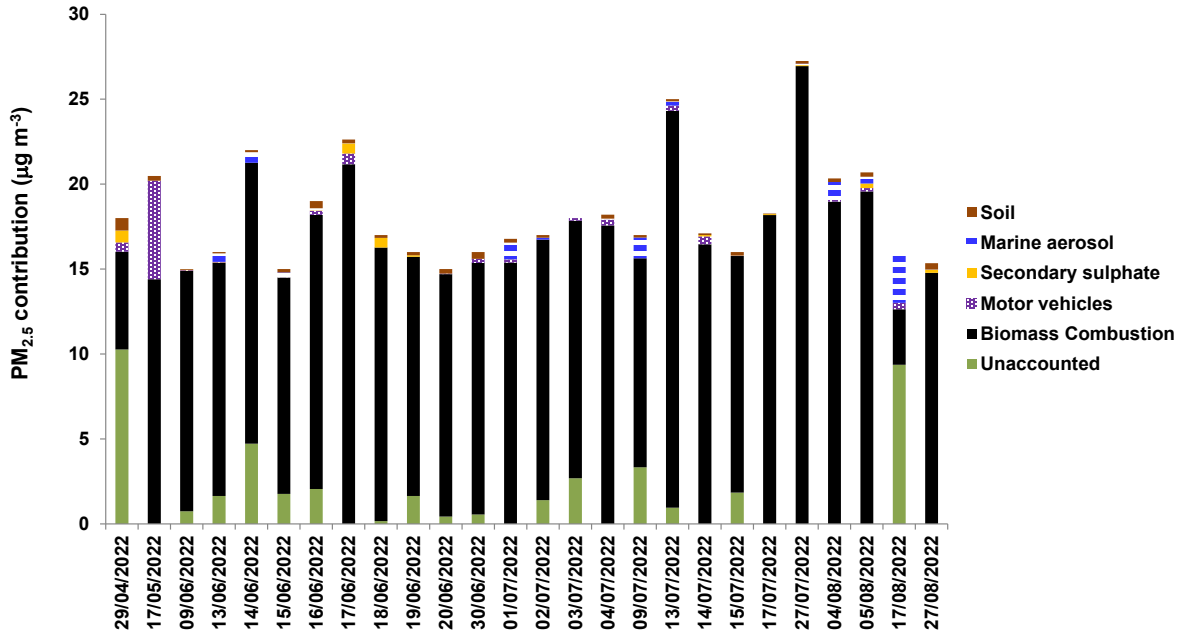

Figure 4.3 Source mass contributions to peak $PM_{2.5}$ events (>15 µg m^{-3}) at Motueka.

Figure 4.3 shows that biomass combustion was responsible for an average of 87% of $PM_{2.5}$ mass on high particulate matter concentration days. The result is consistent with the location of the Motueka monitoring site in a residential area, where solid fuel fires are used for home heating during winter. In New Zealand urban areas, high particulate matter events are generally dominated by biomass burning emissions during winter; concentrations generally peak in the late evening and most (>80%) of the particulate matter is in the fine fraction ($PM_{2.5}$) (Davy et al. 2012; Ancelet et al. 2014, 2015, 2016; Davy and Trompetter 2017, 2020). Interestingly, there were two days (29 April 2022 and 17 October 2022) where the receptor modelling did not account for the majority of $PM_{2.5}$ mass, most likely due to some unmeasured component such as organic matter or secondary nitrate species as discussed in Section 2.3.

During peak winter $PM_{2.5}$ concentrations, contributions from other emission sources were generally low, including any contribution from natural sources (marine aerosol and secondary sulphate).

4.3 Comparison of Source Apportionment with Emissions Inventory Results

An emissions inventory for Motueka has recently been commissioned by TDC. Emissions inventories quantify the amount of contaminants discharged to air either on a mass per day/ month/year or mass per unit area basis and therefore provide a framework for understanding the major emission sources in an airshed. The actual concentrations of those contaminants measured in the airshed will depend on the location of a monitoring site relative to the emission source or the time of day or year that the emissions occur, along with local topography and meteorology – all of which affect the dispersion of pollutants. Emissions from natural sources such as sea salt, windblown dust and natural sources of secondary aerosol are difficult to

quantify due to high uncertainties around specific source emission factors and source activity (i.e. rates of emissions). As such, emissions inventories can be considered complementary to receptor modelling/source apportionment studies, where both anthropogenic and natural source contributions can be quantified (as measured) in the local atmosphere.

The inventory prepared by Environet Limited (Wilson 2023) was designed to assess quantities and sources of discharges to air in Motueka. The sources included were domestic heating, motor vehicles, outdoor burning (including braziers, pizza ovens and solid fuel barbeques) and industrial and commercial activities. The evaluation focused on PM_{10}, $PM_{2.5}$, sulphur oxides, nitrogen oxides and carbon monoxide. Of relevance to this study, the emissions inventory for $PM_{2.5}$ shows that domestic heating (primarily wood fire) emissions dominate both the annual (tonnes/year) and winter (tonnes/day) emissions, as presented in Figure 4.4.

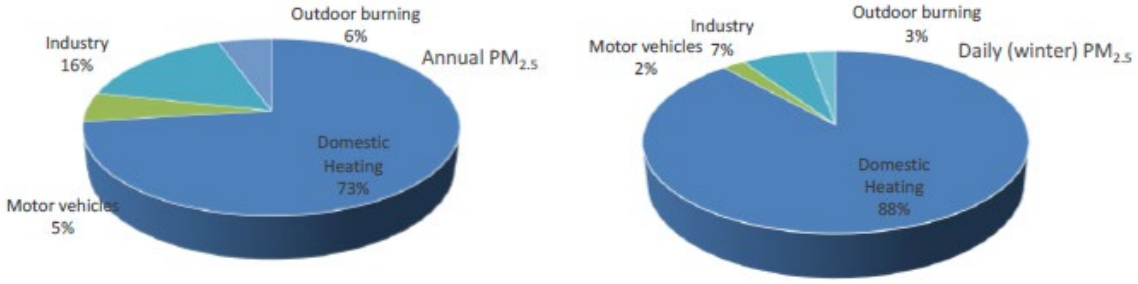

Figure 4.4 Relative contribution of inventoried sources to annual $PM_{2.5}$ (tonnes/year) and daily winter (tonnes/day) $PM_{2.5}$ emissions in Motueka. Source: Wilton (2023).

Figure 4.5 presents the source-apportionment data for annual and winter source contributions to $PM_{2.5}$, which also includes the natural source contributions.

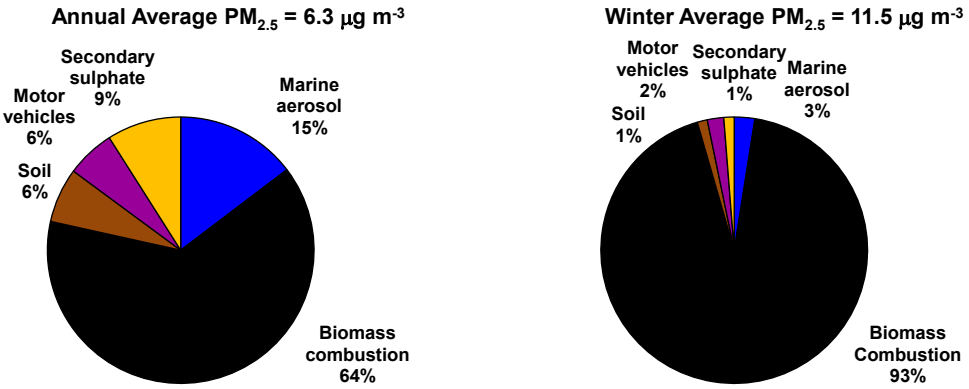

Figure 4.5 Relative contribution of sources to annual $PM_{2.5}$ concentrations and average winter $PM_{2.5}$ concentrations in Motueka (this study).

The differences between the emissions inventory estimates and the source apportionment are that the receptor modelling is based on the ambient concentrations measured at the Ledger Goodman Park site, while the emissions inventory is based on the entire Motueka area. For example, the industry $PM_{2.5}$ emissions are dominated by two activities at Port Motueka several kilometres to the south that are unlikely to impact at the Ledger Goodman Park monitoring site. However, both the emission inventory and receptor modelling show that the primary source affecting $PM_{2.5}$ emissions and the resulting measured $PM_{2.5}$ concentrations is solid fuel fires for domestic space heating during winter, and that the relative contributions estimated by both methods are entirely complimentary. The advantage of having an associated emissions inventory is that TDC can estimate the effect of emission reduction strategies

are likely to have on ambient $PM_{2.5}$ concentrations in order to protect the health of the exposed population.

5.0 SUMMARY OF MOTUEKA PARTICULATE MATTER COMPOSITION AND SOURCE CONTRIBUTIONS

A year-long (January 2022 to January 2023) $PM_{2.5}$ airborne particle sampling programme at Motueka in the Tasman District formed the basis of a study of particulate matter compositional analysis and the attribution of sources contributing to particulate matter concentrations. The particulate matter elemental composition data showed that black carbon, a product of combustion sources, was an important contributor to $PM_{2.5}$ concentrations, along with sodium and chlorine, which were primarily influenced by marine aerosol (sea salt), along with aluminium, silicon and sulphur. $PM_{2.5}$ and black carbon concentrations were found to peak during winter months, indicating that combustion source emissions were likely to be responsible for the higher winter particle concentrations.

Five main source types were extracted from the data by receptor modelling techniques (using PMF); these sources of particulate matter were biomass combustion, motor vehicles, secondary sulphate, marine aerosol and soil. The primary source of peak winter $PM_{2.5}$ in Motueka was the biomass combustion source, which was attributed to the use of solid fuel fires for home heating that contributed 87% of the total $PM_{2.5}$ mass during peak concentrations (greater than 15 μg m^{-3}). The biomass combustion sources associated with home heating emissions were found to be contaminated with As and Pb, which were considered to be due to the use of CCA-treated and old painted timber, respectively.

6.0 ACKNOWLEDGEMENTS

The authors thank Pam Rogers for the filter analytical measurements and Chris Purcell for XRF maintenance.

7.0 REFERENCES

Ancelet T, Davy PK. 2015. Multi-elemental analysis of PM_{10} and apportionment of contributing sources. Lower Hutt (NZ): GNS Science. 10 p. Consultancy Report 2015/117LR. Prepared for Waikato Regional Council.

Ancelet T, Davy PK, Mitchell T, Trompetter WJ, Markwitz A, Weatherburn DC. 2012. Identification of particulate matter sources on an hourly time-scale in a wood burning community. *Environmental Science & Technology*. 46(9):4767–4774. https://doi.org/10.1021/es203937y

Ancelet T, Davy PK, Trompetter WJ, Markwitz A, Weatherburn DC. 2014. Sources and transport of particulate matter on an hourly time-scale during the winter in a New Zealand urban valley. *Urban Climate*. 10:644–655. https://doi.org/10.1016/j.uclim.2014.06.003

Ancelet T, Davy PK, Trompetter WJ. 2015. Particulate matter sources and long-term trends in a small New Zealand city. *Atmospheric Pollution Research*. 6(6):1105–1112. http://dx.doi.org/10.1016/j.apr.2015.06.008

Ashbaugh LL, Malm WC, Sadeh WZ. 1985. A residence time probability analysis of sulfur concentrations at grand Canyon National Park. *Atmospheric Environment (1967)*. 19(8):1263–1270. https://doi.org/10.1016/0004-6981(85)90256-2

Begum BA, Hopke PK, Zhao W. 2005. Source identification of fine particles in Washington, DC, by expanded factor analysis modeling. *Environmental Science & Technology*. 39(4):1129–1137. https://doi.org/10.1021/es049804v

Bennett J, Davy P, Trompetter B, Wang Y, Pierse N, Boulic M, Phipps R, Howden-Chapman P. 2019. Sources of indoor air pollution at a New Zealand urban primary school; a case study. *Atmospheric Pollution Research*. 10(2):435–444. https://doi.org/10.1016/j.apr.2018.09.006

Brimblecombe P. 1986. Air: composition & chemistry. Cambridge (GB): Cambridge University Press. 224 p.

Brown SG, Hafner HR. 2005. Multivariate receptor modelling workbook. Research Triangle Park (NC): United States Environmental Protection Agency.

Brown SG, Eberly S, Paatero P, Norris GA. 2015. Methods for estimating uncertainty in PMF solutions: examples with ambient air and water quality data and guidance on reporting PMF results. *Science of the Total Environment*. 518–519:626–635. https://doi.org/10.1016/j.scitotenv.2015.01.022

Cahill TA, Eldred RA, Motallebi N, Malm WC. 1989. Indirect measurement of hydrocarbon aerosols across the United States by nonsulfate hydrogen-remaining gravimetric mass correlations. *Aerosol Science and Technology*. 10(2):421–429. https://doi.org/10.1080/02786828908959281

Carslaw DC. 2012. The openair manual: open-source tools for analysing air pollution data – manual for version 0.7-0. London (GB): King's College London.

Carslaw DC, Ropkins K. 2012. openair – an R package for air quality data analysis. *Environmental Modelling & Software*. 27–28:52–61. https://doi.org/10.1016/j.envsoft.2011.09.008

Chueinta W, Hopke PK, Paatero P. 2000. Investigation of sources of atmospheric aerosol at urban and suburban residential areas in Thailand by positive matrix factorization. *Atmospheric Environment*. 34(20):3319–3329. https://doi.org/10.1016/S1352-2310(99)00433-1

Cohen D. 1999. Accelerator based ion beam techniques for trace element aerosol analysis. In: Landsberger S, Creatchman M, editors. *Elemental analysis of airborne particles*. Amsterdam (NL): Gordon and Breach Science Publishers. p. 139–196. (Advances in environmental, industrial, and process control technologies; 1).

Cohen D, Taha G, Stelcer E, Garton D, Box G. 2000. The measurement and sources of fine particle elemental carbon at several key sites in NSW over the past eight years. In: *Proceedings of the 15th International Clean Air and Environment Conference*; 2000 Nov 26–30; Sydney, Australia. Mooroolbark (AU): Clean Air Society of Australia and New Zealand. p. 485–490.

Davy PK, Trompetter WJ. 2017. Source apportionment of $PM_{2.5}$ and PM_{10} sources in the Richmond airshed, Tasman District. Lower Hutt (NZ): GNS Science. 69 p. Consultancy Report 2017/86. Prepared for Tasman District Council.

Davy PK, Trompetter WJ. 2018. Heavy metals, black carbon and natural sources of particulate matter in New Zealand. Lower Hutt (NZ): GNS Science. 81 p. Consultancy Report 2017/238. Prepared for Ministry for the Environment.

Davy PK, Trompetter WJ. 2020. Composition, sources and long-term trends for Auckland air particulate matter: summary report. Lower Hutt (NZ): GNS Science. 32 p. + appendices. Consultancy Report 2019/151. Prepared for Auckland Council.

Davy PK, Ancelet T, Trompetter WJ, Markwitz A, Weatherburn DC. 2012. Composition and source contributions of air particulate matter pollution in a New Zealand suburban town. *Atmospheric Pollution Research*. 3(1):143–147. https://doi.org/10.5094/APR.2012.014

Davy PK, Ancelet T, Trompetter WJ, Markwitz A. 2014. Arsenic and air pollution in New Zealand. In: Litter MI, Nicolli HB, Meichtry M, Quici N, Bundschuh J, Bhattacharya P, Naidu R, editors. *One century of the discovery of arsenicosis in Latin America (1914–2014), As 2014: proceedings of the 5th International Congress on Arsenic in the Environment*; 2014 May 11–16; Buenos Aires, Argentina. Boca Raton (FL): CRC Press. p. 394–395.

Davy PK, Ancelet T, Trompetter WJ. 2016. Source apportionment of $PM_{2.5}$ and $PM_{10–2.5}$ samples from St Albans, Christchurch. Lower Hutt (NZ): GNS Science. 61 p. Consultancy Report 2016/72. Prepared for Environment Canterbury.

Dirks KN, Chester A, Salmond JA, Talbot N, Thornley S, Davy P. 2020. Arsenic in hair as a marker of exposure to smoke from the burning of treated wood in domestic wood burners. *International Journal of Environmental Research and Public Health*. 17(11):3944. https://doi.org/10.3390/ijerph17113944

Eberly SI. 2005. EPA PMF 1.1 User's Guide. Washington (DC): United States Environmental Protection Agency. EPA/600/R-06/166.

Fine PM, Cass GR, Simoneit BRT. 2001. Chemical characterization of fine particle emissions from fireplace combustion of woods grown in the northeastern United States. *Environmental Science & Technology*. 35(13):2665–2675. https://doi.org/10.1021/es001466k

Fitzgerald JW. 1991. Marine aerosols: a review. *Atmospheric Environment Part A General Topics*. 25(3–4):533–545. https://doi.org/10.1016/0960-1686(91)90050-H

Grange SK, Salmond JA, Trompetter WJ, Davy PK, Ancelet T. 2013. Effect of atmospheric stability on the impact of domestic wood combustion to air quality of a small urban township in winter. *Atmospheric Environment*. 70:28–38. https://doi.org/10.1016/j.atmosenv.2012.12.047

Hopke PK. 1999. An introduction to source receptor modeling. In: Landsberger S, Creatchman M, editors. *Elemental analysis of airborne particles*. Amsterdam (NL): Gordon and Breach Science Publishers. p. 273–315. (Advances in environmental, industrial, and process control technologies; 1).

Hopke PK. 2003. Recent developments in receptor modeling. *Journal of Chemometrics*. 17(5):255–265. https://doi.org/10.1002/cem.796

Hopke PK, Xie Y, Paatero P. 1999. Mixed multiway analysis of airborne particle composition data. *Journal of Chemometrics*. 13(3–4):343–352. https://doi.org/10.1002/(SICI)1099-128X(199905/08)13:3/4<343::AID-CEM550>3.0.CO;2-P

Horvath H. 1993. Atmospheric light absorption: a review. *Atmospheric Environment Part A General Topics*. 27(3):293–317. https://doi.org/10.1016/0960-1686(93)90104-7

Horvath H. 1997. Experimental calibration for aerosol light absorption measurements using the integrating plate method – summary of the data. *Journal of Aerosol Science*. 28(7):1149–1161. https://doi.org/10.1016/S0021-8502(97)00007-4

Hyslop NP, Trzepla K, Yatkin S, White WH, Ancelet T, Davy P, Butler O, Gerboles M, Kohl S, McWilliams A, et al. 2019. An inter-laboratory evaluation of new multi-element reference materials for atmospheric particulate matter measurements. *Aerosol Science and Technology*. 53(7):771–782. https://doi.org/10.1080/02786826.2019.1606413

Jacobson MC, Hansson HC, Noone KJ, Charlson RJ. 2000. Organic atmospheric aerosols: review and state of the science. *Reviews of Geophysics*. 38(2):267–294. https://doi.org/10.1029/1998RG000045

Jeong C-H, Hopke PK, Kim E, Lee D-W. 2004. The comparison between thermal-optical transmittance elemental carbon and Aethalometer black carbon measured at multiple monitoring sites. *Atmospheric Environment*. 38(31):5193–5204. https://doi.org/10.1016/j.atmosenv.2004.02.065

Kara M, Hopke P, Dumanoglu Y, Altiok H, Elbir T, Odabasi M, Bayram A. 2015. Characterization of PM using multiple site data in a heavily industrialized region of Turkey. *Aerosol and Air Quality Research*. 15(1):11–27. https://doi.org/10.4209/aaqr.2014.02.0039

Khalil MAK, Rasmussen RA. 2003. Tracers of wood smoke. *Atmospheric Environment*. 37(9):1211–1222. https://doi.org/10.1016/S1352-2310(02)01014-2

Kim E, Hopke PK, Edgerton ES. 2003. Source identification of Atlanta aerosol by positive matrix factorization. *Journal of the Air & Waste Management Association*. 53(6):731–739. https://doi.org/10.1080/10473289.2003.10466209

Kim E, Hopke PK, Larson TV, Maykut NN, Lewtas J. 2004. Factor analysis of Seattle fine particles. *Aerosol Science and Technology*. 38(7):724–738. https://doi.org/10.1080/02786820490490119

Lee E, Chan CK, Paatero P. 1999. Application of positive matrix factorization in source apportionment of particulate pollutants in Hong Kong. *Atmospheric Environment*. 33(19):3201–3212. https://doi.org/10.1016/S1352-2310(99)00113-2

Lee JH, Yoshida Y, Turpin BJ, Hopke PK, Poirot RL, Lioy PJ, Oxley JC. 2002. Identification of sources contributing to Mid-Atlantic regional aerosol. *Journal of the Air & Waste Management Association*. 52(10):1186–1205. https://doi.org/10.1080/10473289.2002.10470850

Malm WC, Sisler JF, Huffman D, Eldred RA, Cahill TA. 1994. Spatial and seasonal trends in particle concentration and optical extinction in the United States. *Journal of Geophysical Research: Atmospheres*. 99(D1):1347–1370. https://doi.org/10.1029/93jd02916

Ministry for the Environment. 1997. Environmental performance indicators: proposals for air, freshwater and land. Wellington (NZ): Ministry for the Environment.

Ministry for the Environment. 2011. 2011 users' guide to the revised National Environmental Standards for Air Quality: updated 2014. Wellington (NZ): Ministry for the Environment. 139 p.

Norris G, Duvall R, Brown S, Bai S. 2014. EPA Positive Matrix Factorization (PMF) 5.0 fundamentals and user guide. Washington (DC): US Environmental Protection Agency. 124 p. EPA/600/R-14/108.

Paatero P. 1997. Least squares formulation of robust non-negative factor analysis. *Chemometrics and Intelligent Laboratory Systems*. 37(1):23–35. https://doi.org/10.1016/S0169-7439(96)00044-5

Paatero P, Hopke PK. 2002. Utilizing wind direction and wind speed as independent variables in multilinear receptor modeling studies. *Chemometrics and Intelligent Laboratory Systems*. 60(1):25–41. https://doi.org/10.1016/S0169-7439(01)00183-6

Paatero P, Hopke PK. 2003. Discarding or downweighting high-noise variables in factor analytic models. *Analytica Chimica Acta*. 490(1):277–289. https://doi.org/10.1016/S0003-2670(02)01643-4

Paatero P, Hopke PK, Song X-H, Ramadan Z. 2002. Understanding and controlling rotations in factor analytic models. *Chemometrics and Intelligent Laboratory Systems*. 60(1):253–264. https://doi.org/10.1016/S0169-7439(01)00200-3

Paatero P, Hopke PK, Begum BA, Biswas SK. 2005. A graphical diagnostic method for assessing the rotation in factor analytical models of atmospheric pollution. *Atmospheric Environment*. 39(1):193–201. https://doi.org/10.1016/j.atmosenv.2004.08.018

Paatero P, Eberly S, Brown SG, Norris GA. 2014. Methods for estimating uncertainty in factor analytic solutions. *Atmospheric Measurement Techniques*. 7(3):781–797. https://doi.org/10.5194/amt-7-781-2014

Patel H, Talbot N, Salmond J, Dirks K, Xie S, Davy P. 2020. Implications for air quality management of changes in air quality during lockdown in Auckland (New Zealand) in response to the 2020 SARS-CoV-2 epidemic. *Science of the Total Environment*. 746:141129. https://doi.org/10.1016/j.scitotenv.2020.141129

Ramadan Z, Eickhout B, Song X-H, Buydens LMC, Hopke PK. 2003. Comparison of Positive Matrix Factorization and Multilinear Engine for the source apportionment of particulate pollutants. *Chemometrics and Intelligent Laboratory Systems*. 66(1):15–28. https://doi.org/10.1016/S0169-7439(02)00160-0

Salma I, Chi X, Maenhaut W. 2004. Elemental and organic carbon in urban canyon and background environments in Budapest, Hungary. *Atmospheric Environment*. 38(1):27–36. https://doi.org/10.1016/j.atmosenv.2003.09.047

Scott A. 2014. Timaru source apportionment study. Christchurch (NZ): Environment Canterbury Regional Council. Technical Report R12/100. 30 p.

Seinfeld JH, Pandis SN. 2006. Atmospheric chemistry and physics: from air pollution to climate change. 2nd ed. Hoboken (NJ): John Wiley. 1203 p.

Song X-H, Polissar AV, Hopke PK. 2001. Sources of fine particle composition in the northeastern US. *Atmospheric Environment*. 35(31):5277–5286. https://doi.org/10.1016/S1352-2310(01)00338-7

R Core Team. 2015. R: a language and environment for statistical computing. Vienna (AT): R Foundation for Statistical Computing.

Trompetter WJ. 2004. Ion Beam Analysis results of air particulate filters from the Wellington Regional Council. Lower Hutt (NZ): Institute of Geological & Nuclear Sciences. 17 p. Client Report 2004/24. Prepared for Wellington Regional Council.

Trompetter WJ, Davy PK, Markwitz A. 2010. Influence of environmental conditions on carbonaceous particle concentrations within New Zealand. *Journal of Aerosol Science*. 41(1):134–142. https://doi.org/10.1016/j.jaerosci.2009.11.003

Watson JG, Chow JC, Frazier CA. 1999. X-ray fluorescence analysis of ambient air samples. In: Landsberger S, Creatchman M, editors. *Elemental analysis of airborne particles*. Amsterdam (NL): Gordon and Breach Science Publishers. p. 67–96. (Advances in environmental, industrial, and process control technologies; 1).

Watson JG, Zhu T, Chow JC, Engelbrecht J, Fujita EM, Wilson WE. 2002. Receptor modeling application framework for particle source apportionment. *Chemosphere*. 49(9):1093–1136. https://doi.org/10.1016/S0045-6535(02)00243-6

[WHO] World Health Organization. 2021. WHO global air quality guidelines: particulate matter ($PM_{2.5}$ and PM_{10}), ozone, nitrogen dioxide, sulfur dioxide and carbon monoxide. Bonn (DE): World Health Organization. 273 p.

Wilson E. 2023. Motueka air emissions inventory 2023. Christchurch (NZ): Environet Limited. 36 p.

Yatkin S, Trzepla K, Hyslop NP, White WH, Butler O, Ancelet T, Davy P, Gerboles M, Kohl SD, McWilliams A, et al. 2020. Comparison of a priori and interlaboratory-measurement-consensus approaches for value assignment of multi-element reference materials on PTFE filters. *Microchemical Journal*. 158:105225. https://doi.org/10.1016/j.microc.2020.105225

APPENDICES

This page left intentionally blank.

APPENDIX 1 ANALYSIS TECHNIQUES

A1.1 X-Ray Fluorescence Spectroscopy

X-ray fluorescence spectroscopy (XRF) was used to measure elemental concentrations in $PM_{2.5}$ samples collected on PTFE filters at Motueka. XRF measurements in this study were carried out at the GNS Science XRF facility, and the spectrometer used was a PANalytical Epsilon 5 (PANalytical, the Netherlands). The Epsilon 5 is shown in Figure A1.1. XRF is a non-destructive and relatively rapid method for the elemental analysis of particulate matter samples.

Figure A1.1 The PANalytical Epsilon 5 spectrometer.

XRF is based on the measurement of characteristic X-rays produced by the ejection of an inner shell electron from an atom in the sample, creating a vacancy in the inner atomic shell. A higher-energy electron then drops into the lower-energy orbital and releases a fluorescent X-ray to remove excess energy (Watson et al. 1999). The energy of the released X-ray is characteristic of the emitting element, and the area of the fluorescent X-ray peak (intensity of the peak) is proportional to the number of emitting atoms in the sample. From the intensity, it is possible to calculate a specific element's concentration by direct comparison with standards.

To eject inner shell electrons from atoms in a sample, the XRF spectrometer at GNS Science uses a 100 kV Sc/W X-ray tube. The 100 kV X-rays produced by this tube are able to provide elemental information for elements from Na–U. Unlike ion beam analysis techniques, which are similar to XRF, the PANalytical Epsilon 5 is able to use characteristic K-lines produced by each element for quantification. This is crucial for optimising limits of detection because K-lines have higher intensities and are located in less crowded regions of the X-ray spectrum.

The X-rays emitted by the sample are detected using a high-performance Ge detector, which further improves the detection limits. Figure A1.2 presents a sample X-ray spectrum.

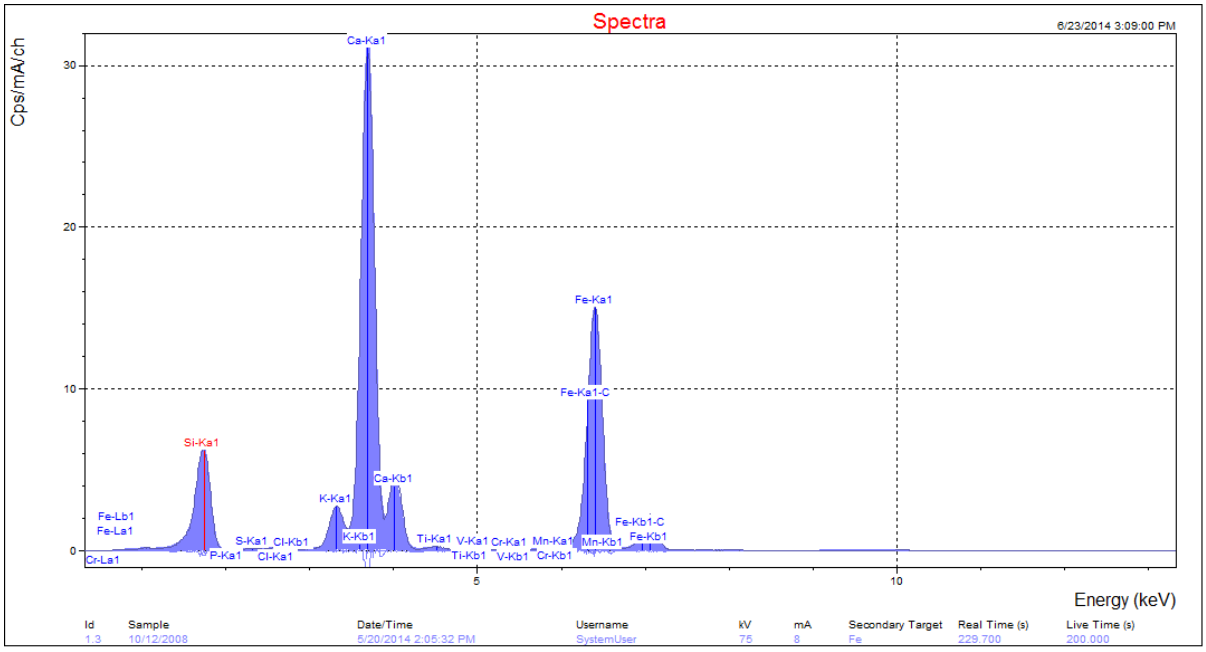

Figure A1.2 Example X-ray spectrum from a PM_{10} sample.

In this study, calibration standards for each of the elements of interest were analysed prior to the samples being run. Once the calibration standards were analysed, spectral deconvolutions were performed using PANalytical software to correct for line overlaps and ensure that the spectra were accurately fit. Calibration curves for each element of interest were produced and used to determine the elemental concentrations from the Motueka samples. Multi-elemental reference standards were also analysed to ensure that the results obtained were robust and accurate (Hyslop et al. 2019; Yatkin et al. 2020).

A1.2 Black Carbon Measurements

Black carbon has been studied extensively, but it is still not clear to what degree it is elemental carbon [(or graphitic) C(0)], high molecular weight refractory weight organic species, or a combination of both (Jacobson et al. 2000). Current literature suggests that black carbon is likely a combination of both, and that, for combustion sources such as petrol- and diesel-fuelled vehicles and biomass combustion (wood burning, coal burning), elemental carbon and organic carbon compounds are the principle aerosol components emitted (Jacobson et al. 2000; Fine et al. 2001; Watson et al. 2002; Salma et al. 2004).

Determination of carbon (soot) on filters was performed by light reflection to provide the black carbon concentration. The absorption and reflection of visible light on particles in the atmosphere or collected on filters is dependent on the particle concentration, density, refractive index and size. For atmospheric particles, black carbon is the most highly absorbing component in the visible light spectrum, with very much smaller components coming from soils, sulphates and nitrate (Horvath 1993, 1997). Hence, to the first order, it can be assumed that all the absorption on atmospheric filters is due to black carbon. The main sources of atmospheric black carbon are anthropogenic combustion sources and include biomass burning, motor vehicles and industrial emissions (Cohen et al. 2000). Cohen and co-workers found that black carbon is typically 10–40% of the fine mass ($PM_{2.5}$) fraction in many urban areas of Australia.

When measuring black carbon by light reflection/transmission, light from a light source is transmitted through a filter onto a photocell. The amount of light absorption is proportional to the amount of black carbon present and provides a value that is a measure of the black carbon on the filter. Conversion of the absorbance value to an atmospheric concentration value of black carbon (BC) requires the use of an empirically derived equation (Cohen et al. 2000):

$$BC\ (\mu g\ cm^{-2}) = (100/2(F\varepsilon))\ ln[R_0/R] \qquad \text{Equation A1.1}$$

where:

- ε is the mass absorbent coefficient for black carbon ($m^2\ g^{-1}$) at a given wavelength.
- $F$is a correction factor to account for other absorbing factors such as sulphates, nitrates, shadowing and filter loading. These effects are generally assumed to be negligible and F is set at 1.00.
- R_0, R are the pre- and post-reflection intensity measurements, respectively.

Black carbon was measured at GNS Science using the M43D Digital Smoke Stain Reflectometer. The following equation (from Willy Maenhaut, Institute for Nuclear Sciences, University of Gent Proeftuinstraat 86, B-9000 GENT, Belgium) was used for obtaining black carbon from reflectance measurements on Nucleopore polycarbonate filters or Pall Life Sciences Teflon filters:

$$BC\ (\mu g\ cm^{-2}) = [1000 \times LOG(R_{blank}/R_{sample}) + 2.39] / 45.8 \qquad \text{Equation A1.2}$$

Where R_{blank} is the average reflectance for a series of blank filters; R_{blank} is close (but not identical) to 100. GNS Science always use the same blank filter for adjusting to 100 and R_{sample} is the reflectance for a filter sample (normally lower than 100)

with 2.39 and 45.8 constants derived using a series of 100 Nuclepore polycarbonate filter samples, which served as secondary standards; the black carbon loading (in μg cm^{-2}) for these samples had been determined by Prof. Dr. M.O. Andreae (Max Planck Institute of Chemistry, Mainz, Germany) relative to standards that were prepared by collecting burning acetylene soot on filters and determining the mass concentration gravimetrically (Trompetter 2004).

A1.3 Positive Matrix Factorization

Positive matrix factorisation (PMF) is a linear least-squares approach to factor analysis and was designed to overcome the receptor modeling problems associated with techniques like principal components analysis (PCA) and the *a priori* knowledge required for chemical mass balance approaches (Paatero et al. 2005). With PMF, sources are constrained to have non-negative species concentrations, no sample can have a negative source contribution and error estimates for each observed data point are used as point-by-point weights. This feature is a distinct advantage, in that it can accommodate missing and below detection limit data that is a common feature of environmental monitoring results (Song et al. 2001). In fact, the signal-to-noise ratio for an individual elemental measurement can have a significant influence on a receptor model and modeling results. For the weakest (closest to detection limit) species, the variance may be entirely from noise (Paatero and Hopke 2002). Paatero and Hopke strongly suggest down-weighting or discarding noisy variables that are always below their detection limit or species that have a lot of error in their measurements relative to the magnitude of their concentrations (Paatero and Hopke 2003). The distinct advantage of PMF is that mass concentrations can be included in the model and the results are directly interpretable as mass contributions from each factor (source).

A1.3.1 PMF Model Outline

The mathematical basis for PMF is described in detail by Paatero (Paatero 1997). Briefly, PMF uses a weighted least-squares fit with the known error estimates of measured elemental concentrations used to derive the weights. In matrix notation this is indicated as:

$$X = GF + E \qquad \text{Equation A1.3}$$

where:

- X is the known n x m matrix of m measured elemental species in n samples.
- G is an n x p matrix of source contributions to the samples.
- F is a p x m matrix of source compositions (source profiles).
- E is a residual matrix – the difference between measurement X and model Y.
- E can be defined as a function of factors G and F.

$$e_{ij} = x_{ij} - y_{ij} = x_{ij} - \sum_{k=1}^{p} g_{ik} f_{kj} \qquad \text{Equation A1.4}$$

where:

- i = 1,……,n elements.
- j = 1,……,m samples.
- k = 1,…...,p sources.

PMF constrains all elements of G and F to be non-negative, meaning that elements cannot have negative concentrations and samples cannot have negative source contributions, as in real space. The task of PMF is to minimise the function Q such that:

$$Q(E) = \sum_{i=1}^{n} \sum_{j=1}^{m} (e_{ik} / \sigma_{kj})^2 \qquad \text{Equation A1.5}$$

where σ_{ij} is the error estimate for x_{ij}. Another advantage of PMF is the ability to handle extreme values typical of air-pollutant concentrations, as well as true outliers that would normally skew PCA. In either case, such high values would have significant influence on the solution (commonly referred to as leverage). PMF has been successfully applied to receptor modeling studies in a number of countries around the world (Hopke et al. 1999; Lee et al. 1999; Chueinta et al. 2000; Song et al. 2001, Lee et al. 2002; Kim et al. 2003, 2004; Jeong et al. 2004; Begum et al. 2005), including New Zealand (Davy et al. 2012; Ancelet et al. 2012, 2014; Bennett et al. 2019; Davy and Trompetter 2020; Patel et al. 2020).

A1.3.2 PMF Model Used

Two programs have been written to implement different algorithms for solving the least squares PMF problem; these are PMF2 and EPAPMF, which incorporates the Multilinear Engine (ME-2) (Hopke et al. 1999; Ramadan et al. 2003). In effect, the EPAPMF program provides a more flexible framework than PMF2 for controlling the solutions of the factor analysis with the ability of imposing explicit external constraints.

This study used EPAPMF 5.0 (version 14.0), which incorporates a graphical user interface (GUI) based on the ME-2 program. Both PMF2 and EPAPMF programs can be operated in a robust mode, meaning that 'outliers' are not allowed to overly influence the fitting of the contributions and profiles (Eberly 2005). The user specifies two input files, one file with the concentrations and one with the uncertainties associated with those concentrations. The methodology for developing an uncertainty matrix associated with the elemental concentrations for this work is discussed in Section A1.4.2.

A1.3.3 PMF Model Inputs

The PMF programs provide the user with a number of choices in model parameters that can influence the final solution. Two parameters, the 'signal-to-noise ratio' and the 'species category' are of particular importance and are described below.

Signal-to-noise ratio (S/N): This is a useful diagnostic statistic estimated from the input data and uncertainty files. Two calculations are performed to determine S/N, where concentrations below uncertainty are determined to have no signal, and, for concentrations above uncertainty, the difference between concentration (x_i) and uncertainty (s_i) is used as the signal.

$$d_{ij} = \left(\frac{x_{ij} - s_{ij}}{s_{ij}} \right) \quad \text{if } x_{ij} > s_{ij}$$

$$d_{ij} = 0 \qquad \text{if } x_{ij} \leq s_{ij}$$

S/N is then calculated using Equation A1.6:

$$\left(\frac{S}{N} \right)_j = 1/n \sum_{i=1}^{n} d_{ij} \qquad \text{Equation A1.6}$$

The result with this S/N calculation is that species with concentrations always below their uncertainty have a S/N of 0. Species with concentrations that are twice the uncertainty value have a S/N of 1. S/N greater than 1 may often indicate a species with 'good' signal, although this depends on how uncertainties were determined. Negative concentration values do not contribute to the S/N, and species with a handful of high concentration events will not have artificially high S/N (Norris et al. 2014).

Species category: This enables the user to specify whether the elemental species should be considered:

- Strong – whereby the element is generally present in concentrations well above the limit of detection (LOD) (high signal-to-noise ratio) and the uncertainty matrix is a reasonable representation of the errors.
- Weak – where the element may be present in concentrations near the LOD (low signal-to-noise ratio); there is doubt about some of the measurements and/or error estimates; or the elemental species is only detected some of the time. If 'Weak' is chosen, EPAPMF increases the user-provided uncertainties for that variable by a factor of 3.
- Bad – that variable is excluded from the model run.

For this work, an element with concentrations at least three times above the LOD, a high signal-to-noise ratio (>2) and that was present in all samples was generally considered to be 'Strong'. Variables were labelled as weak if their concentrations were generally low, had a low signal to noise ratio, were only present in a few samples or there was a lower level of confidence in their measurement. Mass concentration gravimetric measurements and black carbon were also down-weighted as 'Weak' depending on the dataset, as their concentrations are generally several orders of magnitude above other species, which can have the tendency to 'pull' the model. Paatero and Hopke (2003) recommend that such variables be down-weighted and that it does not particularly affect the model fitting if those variables are from real sources. What does affect the model severely is if a dubious variable is over-weighted. Elements that had a low signal-to-noise ratio (<0.5) were examined using bivariate correlation plots to determine inter-species relationships. Those low S/N variables with little or no association with other species, that had mostly zero values, or were doubtful for any reason, were labelled as 'Bad' and subsequently not included in the analyses.

If the model is appropriate for the data and if the uncertainties specified are truly reflective of the uncertainties in the data, then *Q* (according to Eberly [2005]) should be approximately equal to the number of data points in the concentration dataset:

$$Theoretical\ Q = \#\ samples \times \#\ species\ measured \qquad \text{Equation A1.7}$$

However, a slightly different approach to calculating the Theoretical *Q* value was recommended (Brown and Hafner 2005), which takes into account the degrees of freedom in the PMF model and the additional constraints in place for each model run. This theoretical *Q* calculation Q_{th} is given as:

$$Q_{th} = (\#\ samples \times \#\ good\ species) + [(\#\ samples \times \#\ weak\ species)/3] - (\#\ samples \times factors\ estimated) \qquad \text{Equation A1.8}$$

Both approaches have been taken into account for this study, and it is likely that the actual value lies somewhere between the two. Further guidance has more recently been provided by Paatero et al. (2014) and Brown et al. (2015), where a third parameter, $Q_{expected}$, should also be calculated but only the 'good' or non-weak variables taken into account:

$$The\ expected\ value\ of\ Q\ is\ approximately = (number\ of\ non\text{-}weak\ data\ values\ in\ X) - (numbers\ of\ elements\ in\ G\ and\ F,\ taken\ together) \qquad \text{Equation A1.9}$$

A down-weighted weak variable has only a small, rarely significant, contribution to $Q_{expected}$ and, for simplicity, is excluded here. If the *Q* value of the chosen model differs significantly from what is expected (e.g. by a factor of 10 or more), then DISP error analysis becomes invalid and BS-DISP is likely questionable.

In PMF, it is assumed that only the x_{ij}'s are known and that the goal is to estimate the contributions (g_{ik}) and factors (or profiles) (f_{kj}). It is assumed that the contributions and mass fractions are all non-negative, hence the 'constrained' part of the least-squares. Additionally, EPAPMF allows the user to say how much uncertainty there is in each x_{ij}. Species-days with lots of uncertainty are not allowed to influence the estimation of the contributions and profiles as much as those with small uncertainty, hence the 'weighted' part of the least squares and the advantage of this approach over PCA.

Diagnostic outputs from the PMF models were used to guide the appropriateness of the number of factors generated and how well the receptor modelling was accounting for the input data. Where necessary, initial solutions have been 'rotated' to provide a better separation of factors (sources) that were considered physically reasonable (Paatero et al. 2002). Each PMF model run reported in this study is accompanied by the modelling statistics, along with comments where appropriate.

A1.4 Dataset Quality Assurance

Quality assurance of sample elemental datasets is vital so that any dubious samples, measurements and outliers are removed, as these will invariably affect the results of receptor modelling. In general, the larger the dataset used for receptor modelling, the more robust the analysis. The following sections describe the methodology used to check data integrity and provide a quality assurance process that ensured the data being used in subsequent factor analysis was as robust as possible.

A1.4.1 Mass Reconstruction and Mass Closure

Once the sample analysis for the range of analytes has been carried out, it is important to check that total measured mass does not exceed gravimetric mass (Cohen 1999). Ideally, when elemental analysis and organic compound analysis has been undertaken on the same sample, one can reconstruct the mass using the following general equation for ambient samples as a first approximation (Cahill et al. 1989; Malm et al. 1994; Cohen 1999):

$$Reconstructed\ mass = [Soil] + [OC] + [BC] + [Smoke] + [Sulphate] + [Seasalt] \quad \text{Equation A1.10}$$

where:

- [Soil] = 2.20[Al] + 2.49[Si] + 1.63[Ca] + 2.42[Fe] + 1.94[Ti]
- [OC] = Σ[Concentrations of organic compounds]
- [BC] = Concentration of black carbon (soot)
- [Smoke] = [K] − 0.6[Fe]
- [Seasalt] = 2.54[Na]
- [Sulphate] = 4.125[S]

The reconstructed mass (RCM) is based on the fact that the six composite variables or 'pseudo' sources given in Equation A1.10 are generally the major contributors to fine and coarse particle mass and are based on geochemical principles and constraints. The [Soil] factor contains elements predominantly found in crustal matter (Al, Si, Ca, Fe, Ti) and includes a multiplier to correct for oxygen content and an additional multiplier of 1.16 to correct for the fact that three major oxide contributors (MgO, K_2O, Na_2O), carbonate and bound water are excluded from the equation.

[BC] is the concentration of black carbon, measured in this case by light reflectance/ absorbance. [Smoke] represents K not included as part of crustal matter and tends to be an indicator of biomass burning.

[Seasalt] represents the marine aerosol contribution and assumes that the NaCl weight is 2.54 times the Na concentration. Na is used, as it is well known that Cl can be volatilised from aerosol or filters in the presence of acidic aerosol, particularly in the fine fraction via the following reactions (Lee et al. 1999):

$$NaCl(p) + HNO_3(ag) \rightarrow NaNO_3(p) + HCL(g)$$

$$2NaCl(p) + H_2SO_4(ag) \rightarrow Na_2SO_4(p) + 2HCL(g)$$

Alternatively, where Cl loss is likely to be minimal, such as in the coarse fraction or for both size fractions near coastal locations and relatively clean air in the absence of acid aerosol, then the reciprocal calculation of [Seasalt] = 1.65[Cl] can be substituted, particularly where Na concentrations are uncertain.

Most fine sulphate particles are the result of oxidation of SO_2 gas to sulphate particles in the atmosphere (Malm et al. 1994). It is assumed that sulphate is present in fully neutralised form as ammonium sulphate. [Sulphate] therefore represents the ammonium sulphate contribution to aerosol mass with the multiplicative factor of 4.125[S] to account for ammonium ion and oxygen mass [i.e. $(NH_4)_2SO_4$ = ((14 + 4)2 + 32 + (16 x 4)/32)].

Additionally, the sulphate component not associated with sea salt can be calculated from Equation A1.11 (Cohen 1999):

$$Non\text{-}sea\ salt\ sulphate\ (NSS\text{-}Sulphate) = 4.125\ ([S_{tot}] - 0.0543[Cl]) \quad \text{Equation A1.11}$$

where the sulphur concentrations contributed by sea salt are inferred from the chlorine concentrations, i.e. [S/Cl] sea salt = 0.0543, and the factor of 4.125 assumes that the sulphate has been fully neutralised and is generally present as $(NH_4)_2SO_4$ (Cahill et al. 1990; Malm et al. 1994; Cohen 1999).

The RCM and mass closure calculations using the pseudo-source and pseudo-element approach are a useful way to examine initial relationships in the data and how the measured mass of species in samples compares to gravimetric mass. Note that some scatter is possible because not all aerosols are necessarily measured and accounted for, such as all organic carbon, ammonium species, nitrates and unbound water.

A1.4.2 Dataset Preparation

Careful preparation of a dataset is required because serious errors in data analysis and receptor modeling results can be caused by erroneous individual data values. The general methodology followed for dataset preparation was as recommended by Brown and Hafner (2005) and the EPAPMF 5.0 User Guide (Norris et al. 2014). For this study, all data were checked for consistency with the following parameters:

- Individual sample collection validation.
- Gravimetric mass validation.
- Analysis of RCM versus gravimetric mass to assess mass closure and linearity.
- Identification of unusual values, including noticeably extreme values and values that normally track with other species (e.g. Al and Si) but deviate in one or two samples. Scatter plots and time-series plots were used to identify unusual values. One-off events such as fireworks displays, forest fires or vegetative burn-offs may affect a receptor model, as it is forced to find a profile that matches only that day;
- Species were included in a dataset if at least 70% of data was above the LOD and signal-to-noise ratios were checked to ensure data had sufficient variability. Important tracers of a source where less than 70% of data was above the LOD were included, but model runs with and without the data were used to assess the effect.

In practise during data analyses, the above steps were a re-iterative process of cross-checking as issues were identified and corrected for, or certain data excluded and the effects of this then studied.

A1.4.2.1 PMF Data Matrix Population

The following steps were followed to produce a final dataset for use in the PMF receptor model (Brown and Hafner 2005).

Below detection limit data: For given values, the reported concentration was used and the corresponding uncertainty checked to ensure that it had a high value.

Missing data: Substituted with the dataset median value for that species.

A1.4.2.2 PMF Uncertainty Matrix Population

Uncertainties can have a large effect on model results, so they must be carefully compiled. The effect of under-estimating uncertainties can be severe, while over-estimating uncertainties does not do too much harm (Paatero and Hopke 2003).

Uncertainties for data: Uncertainties for the XRF elemental data were calculated using the following equations (Kara et al. 2015):

- $\sigma_{ij} = x_{ij} + 2/3(DL_j)$ for samples below limit of detection
- $\sigma_{ij} = 0.2x_{ij} + 2/3(DLj)$; $DL_j < x_{ij} < 3DL_j$ and $\sigma_{ij} = 0.1x_{ij} + 2/3(DL_j)$; $x_{ij} > 3DL_j$ for detected values

where x_{ij} is the determined concentration for species j in the i^{th} sample, and DL_j is the detection limit for species j.

Missing data: Uncertainty was calculated as 4 $\times$ median value over the entire species dataset.

PM gravimetric mass: Uncertainty was given as 4 $\times$ mass value to down-weight the variable.

Re-iterative model runs were used to examine the effect of including species with high uncertainties or low concentrations. In general, it was found that the initial uncertainty estimations were sufficient and that adjusting the ‘additional modelling uncertainty’ function accommodated any issues with modelled variables, such as those with residuals outside ± 3 standard deviations.

APPENDIX 2 MOTUEKA PARTICULATE MATTER DATA ANALYSIS SUMMARY

Using the methodology outlined in Section A1.4.1, Figure A2.1 presents the mass reconstruction results for Motueka $PM_{2.5}$. Figure A2.2 presents a correlation plot matrix for key elemental species. A critical factor in the success of receptor modelling is the ability to reproduce observed versus predicted (modelled) mass. This was clearly being achieved in the case of Motueka $PM_{2.5}$, as presented in Figure A2.3 showing observed versus predicted (modelled) mass.

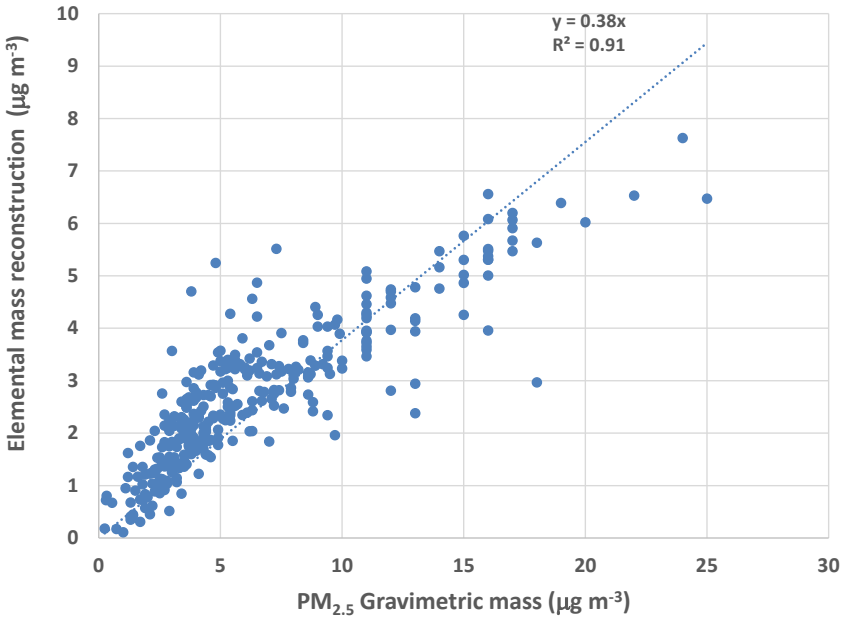

Figure A2.1 Plot of Motueka $PM_{2.5}$ elemental mass reconstruction against gravimetric $PM_{2.5}$ mass.

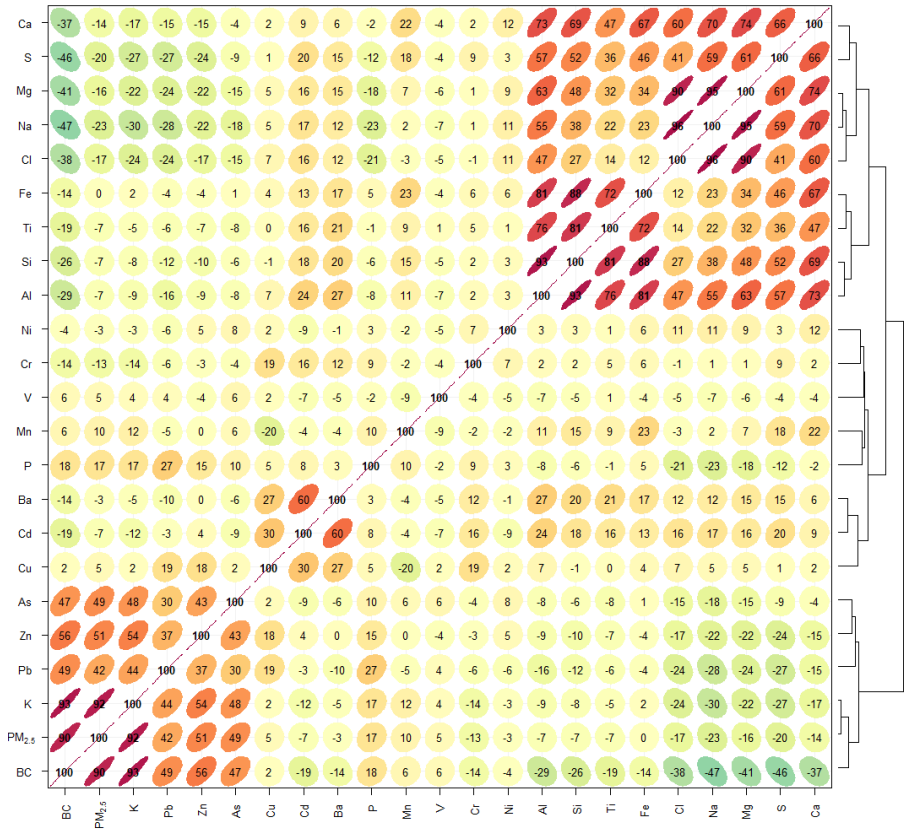

Figure A2.2 Particulate matter and elemental composition correlation plot for Motueka $PM_{2.5}$ samples.

A2.1 Motueka PMF Receptor Modelling Diagnostics

PMF analyses involve many details about the development of the data, decisions of what data to include/exclude, determination of a solution and evaluation of robustness of that solution. The following diagnostics for the PMF solutions are reported as recommended by Paatero et al. (2014) and Brown et al. (2015) and should be read in conjunction with Section 2.1 and Appendix 1.

Table A2.1 Summary of EPAPMF settings for receptor modelling of Motueka $PM_{2.5}$.

Parameter	Setting
Data type; averaging timeframe	$PM_{2.5}$ daily
N samples	327
N factors	5
Treatment of missing data	No missing data
Treatment of data below detection limit (BDL)	Data used as reported, no modification or censoring of BDL data
Lower limit for normalised factor contributions gik	-0.2
Robust mode	Yes
Constraints	None
Seed value	Random
N bootstraps in BS	200
r^2 for BS	0.6

DISP dQmax	4, 8, 16, 32
DISP active species	$PM_{2.5}$, BC, Na, Mg, Al, Si, S, Cl, K, Ca, Ti, Fe, Cu
N bootstraps; r^2 for BS in BS-DISP	200; 0.6
BS-DISP active species	BC, Na, Mg, Al, Si, S, Cl, K, Ca, Ti, Fe, Cu
BS-DISP dQmax	0.5, 1, 2, 4
Extra modelling uncertainty	10%

Table A2.2 Output diagnostics for receptor modelling of Motueka particulate matter.

Diagnostic	Five Factors
$Q_{Theoretical}$	2834
$Q_{Expected}$	2551
Q_{true}	749.023
Q_{robust}	749.026
$Q_{robust}/Q_{expected}$	0.2936
DISP Diagnostics	
Error code	0
Largest Decrease in Q:	0
DISP % dQ	0
DISP swaps by factor	0
BS-DISP Diagnostics	
BS mapping (Fpeak BS) – Unmapped	98% (100%) – 0
BS-DISP % cases accepted	98%
Largest Decrease in Q:	-1.704
BS-DISP % dQ	-0.18962
Number of Decreases in Q:	0
Number of Swaps in Best Fit:	1
Number of Swaps in DISP:	2
BS-DISP swaps by factor	1, 0, 1, 0, 2

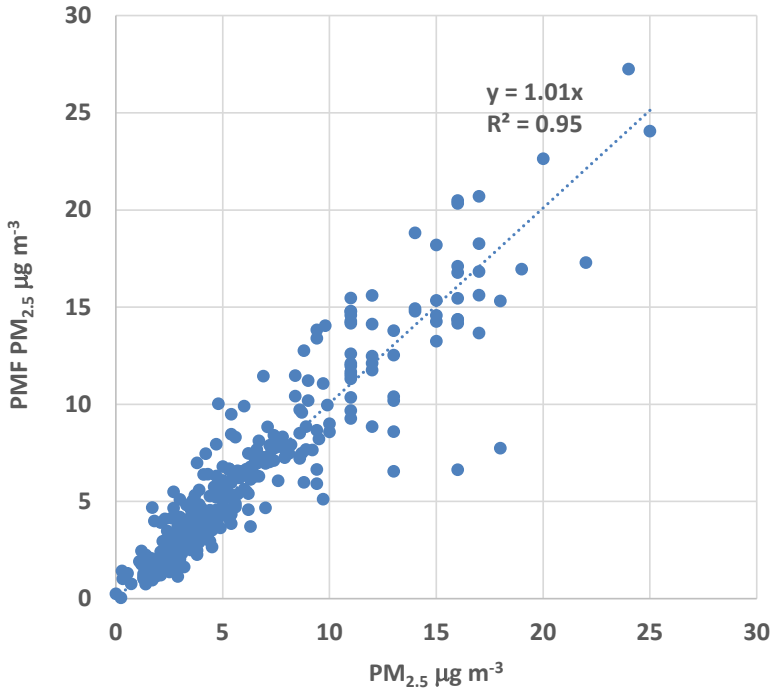

Figure A2.3 Plot of Motueka $PM_{2.5}$ predicted (PMF mass) against observed gravimetric $PM_{2.5}$ mass.